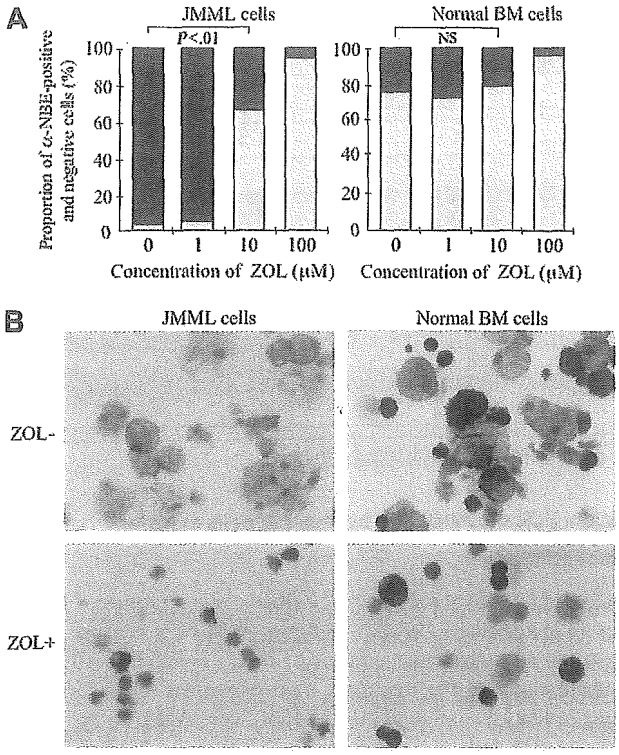

Figure 4. Effect of ZOL on the differentiation of JMML and normal BM cells in the suspension culture. (A) Effect of ZOL on the proportion of α-NBE–positive and –negative cells in the suspension culture of JMML and normal BM cells. Each value indicates the mean calculated from the data for 3 patients with JMML and 3 healthy donors. NS indicates not significant. ▩ indicates α-NBE-positive cells; ▤, α-NBE-negative cells. (B) Appearance of α-NBE–positive and –negative cells in the suspension culture of BM cells of a patient with JMML (case 4) and a healthy donor (case 5) without and with 10 ng/mL GM-CSF (microscope, BH2, Olympus; camera module, DP70, Olympus; objective lens, Span, Olympus; numerical aperture, 0.7; magnification, × 40). α-NBE–positive macrophages possess brown granules in their cytoplasm.

proportion of α-NBE–positive macrophages and α-NBE–negative granulocytes at concentrations of 1 and 10 μM, but, in the culture with 100 μM ZOL, most of the cultured cells were α-NBE–negative granulocytes (Figure 4A-B).

The results in the suspension culture indicate that 100 μM ZOL inhibits the development of both JMML and normal BM cells, but 10 μM ZOL predominantly inhibits the spontaneous proliferation and differentiation along monocyte/macrophage lineage of JMML BM cells.

Flow cytometric analysis of the cells in the suspension culture of JMML and normal BM cells

The effect of ZOL on the differentiation of JMML and normal BM cells in the suspension culture was analyzed by flow cytometry. Figure 5 shows a representative flow cytometric profile of nonerythroid BM cells of a patient with JMML (case 4) before and after 10 days of suspension culture with and without 10 μM ZOL, and Table 2 summarizes the ratio of granulocytes, monocytes/macrophages, lymphocyte, and blastic cells in the population excluding CD45-negative nucleated erythroid cells before and after 10 days of the suspension culture of BM cells from 3 patients with JMML (cases 4, 6, and 7) and 3 healthy donors (cases 1, 3, and 5), which was determined by using SSC and CD45 staining.

Approximately one third of the nonerythroid cells obtained from BM cells of patients with JMML were monocytes/macrophages, characterized by high SSC and bright CD45 expression, which also expressed CD11b, CD13, CD14, CD16, and HLA-DR but no CD34, and half were high SSC and lower-density CD45-expressing granulocytes that were $CD13^+$, $CD16^+$, and $CD33^+$, but $CD14^-$ and $CD34^-$ (Figure 5; Table 2; data not shown). There was also a substantial number of lower SSC and bright CD45-expressing lymphocytes and lower SSC and lower CD45-expressing blastic cells that expressed HLA-DR and CD34 but neither CD11b, CD13, CD14, CD16, nor CD33. When cultured for 10 days, JMML BM cells generated a large number of mature macrophages revealing more bright CD45 expression. Granulocytes accounted for only 2% ± 1%, but 6% ± 2% of the population were blastic cells. On the addition of greater than 10 μM ZOL, however, the production of monocytes/macrophages was significantly suppressed, and the monocyte/macrophage population contained a proportion of lower CD11b-expressing immature monocytes/macrophages. A third of the cultured cells were granulocytes, and a substantial number of blastic cells were still present (8% ± 1%). Nonerythroid cells obtained from normal BM cells consisted of 77% ± 9% granulocytes, 6% ± 4% $CD11b^{bright}$/$HLA\text{-}DR^+$ mature monocytes/macrophages, 12% ± 4% lymphocytes, and a few blastic cells expressing CD34 (Table 2; data not shown). In the culture of normal BM cells with GM-CSF, macrophages also increased, but the percentage was 28% ± 3%. A large number of granulocytes existed, but no or few blastic cells did. The addition of

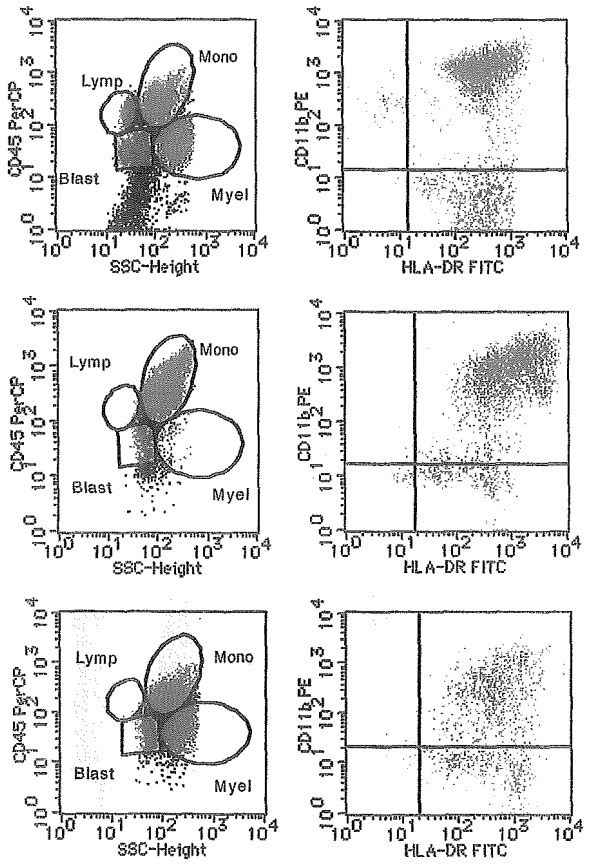

Figure 5. Representative flow cytometric profile of the cells in the suspension culture of JMML BM cells. The nonerythroid BM cells of a patient with JMML (case 4) before (top row) and after 10 days of culture without and with 10 μM ZOL (middle and bottom rows, respectively) were examined by flow cytometry. Populations of granulocytes (Myel, dark blue dots), monocytes/macrophages (Mono, green dots), lymphocytes (Lymp, bright blue dots), and blastic cells (Blast, red dots) were identified by a combination of SSC and CD45 staining (left). CD11b and HLA-DR expression in monocytes/macrophages and blastic cells was further analyzed (right).

Table 2. Proportion of each cell population in nonerythroid cells cultured from JMML and normal BM cells

	ZOL concentration, μM				
	Day 0	Day 10			
	0	0	1	10	100
JMML cells, %					
Granulocytes	46 ± 7	2 ± 1	3 ± 2	30 ± 7	43 ± 5
Monocytes/macrophages	30 ± 9	92 ± 2	88 ± 6	62 ± 9	51 ± 9
Lymphocytes	11 ± 2	0 ± 0	0 ± 0	0 ± 0	0 ± 0
Blasts	13 ± 4	6 ± 2	9 ± 4	8 ± 1	6 ± 2
Normal BM cells, %					
Granulocytes	77 ± 9	68 ± 9	69 ± 7	62 ± 6	75 ± 3
Monocytes/macrophages	6 ± 4	28 ± 3	26 ± 4	38 ± 6	25 ± 3
Lymphocytes	12 ± 4	4 ± 5	5 ± 4	0 ± 0	0 ± 0
Blasts	5 ± 1	0 ± 0	0 ± 0	0 ± 0	0 ± 0

Each value (mean ± SD) was calculated from data for 3 patients with JMML (cases 4, 6, and 7) and healthy donors (cases 1, 3, and 5).

ZOL did not have a significant effect on the composition of the population cultured from normal BM cells.

Thus, 10 μM ZOL affected the predominant differentiation along monocyte/macrophage lineage of JMML BM cells but not the development of normal BM cells. Furthermore, although 10 μM ZOL inhibited the massive expansion of mature monocytes/macrophages, an immature population of JMML cells survived.

Effect of ZOL on clonal cells derived from JMML BM cells

To confirm the inhibitory effect of ZOL on JMML BM cells, we carried out suspension culture of clonal cells derived from single spontaneous colonies formed in culture of BM cells of a patient with JMML (case 4). Five spontaneous colonies containing 100 to 200 cells generated from the JMML BM sample at day 5 of clonal culture were randomly chosen, individually removed, and divided equally. Each half was incubated in a suspension culture with or without 10 μM ZOL for 10 days. In all 5 colonies examined, the number of cells generated with ZOL was approximately a tenth of that without ZOL. At 10 μM, ZOL also affected the differentiation of clonal cells derived from the same clones (Figure 6). Most of the cells contained in the half cultured without ZOL were macrophages (99% ± 0%), whereas the half with 10 μM ZOL contained a substantial number of granulocytes in all 5 experiments (6% ± 3%). This result clearly indicates that 10 μM ZOL inhibits the proliferation and differentiation along monocyte/macrophage lineage of JMML cells at a clone level.

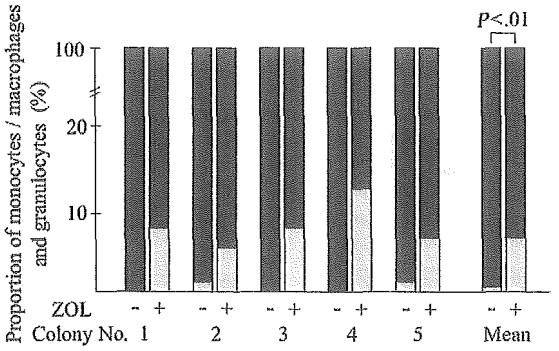

Figure 6. Effect of ZOL on the clonal cells derived from single spontaneous colonies in the culture of JMML BM cells. Five spontaneous colonies generated from BM cells of 3 patients with JMML at day 5 of clonal culture were individually lifted and divided equally, then each half was incubated in the suspension culture with or without 10 μM ZOL for 10 days. The proportion of monocytes/macrophages and granulocytes was determined on cytospin smears of the cultured cells cytochemically stained with α-NBE. ■ indicates monocytes/ macrophages; ▨, granulocytes.

Effect of ZOL on JMML and normal BM cells at lower concentrations

Finally, we examined the effect of ZOL at concentrations of 1 to 10 μM on the growth of JMML and normal BM cells because it was shown that the serum concentration of ZOL was less than 10 μM in a clinical study of the treatment of osteoporosis.[26] As shown in Figure 7, when 1, 3, 6, and 10 μM ZOL were added to the clonal culture of BM cells of a patient with JMML (case 7), the number and size of spontaneous colonies were depressed at concentrations of more than 3 μM ZOL. The number of spontaneous GM colonies significantly decreased and that of G colonies increased even at 3 μM ZOL ($P < .05$). By contrast, 3 μM ZOL had little effect on the colony formation from normal BM cells (case 6) by 10 ng/mL GM-CSF.

Discussion

BM cells of all 8 patients with JMML enrolled in this study produced spontaneous colonies in the culture without hematopoietic factors in accordance with previous reports.[8,36] Because normal BM cells generated no colonies under the same condition, the spontaneous colonies were considered to be derived from the abnormal JMML clones. The several studies showed that the spontaneous colony formation by JMML cells is caused by hypersensitivity to GM-CSF through various molecular mechanisms continuously activating the GM-CSFR–RAS signal transduction pathway.[10,11,15] Our findings, that the number of spontaneous colonies was comparable to that of colonies formed in the presence

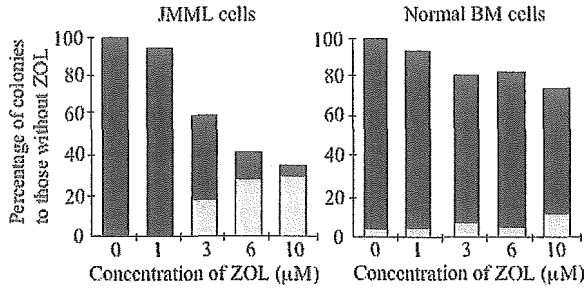

Figure 7. Effect of ZOL on the colony formation from JMML and normal BM cells at less than 10 μM. BM cells of a patient with JMML (case 7) and a healthy adult (case 6) were incubated in the clonal culture with concentrations of 0, 1, 3, 6, and 10 μM ZOL for 14 days in the absence and presence of GM-CSF (10 ng/mL), respectively. ■ indicates GM colonies; ▨, G colonies.

of GM-CSF in most patients with JMML and that there was no remarkable difference in the inhibitory effects of ZOL, a RAS-blocking compound, between the colony formation from JMML cells with and without GM-CSF, are consistent with these studies. In the present study, however, the number of spontaneous colonies varied among patients with JMML. For example, the number was relatively small in cases 3 and 6, in both of which the number of colonies increased to more than 2-fold with the addition of GM-CSF to the culture.

Most of the spontaneous colonies were GM colonies consisting of both macrophages and granulocytes. We also observed that 10 μM ZOL induced the emergence of a significant number of erythroid colonies from JMML cells in the presence of only erythropoietin (Y.O., A.M., H.K., Feng Ma, T.T., and K.T., manuscript in preparation). These observations indicate the multipotentiality of JMML clones.[8] However, the proportion of macrophages in the spontaneous GM colonies derived from JMML cells was higher than that in GM colonies induced from normal BM cells by GM-CSF. Furthermore, the proportion of macrophages in the suspension culture of JMML BM cells was also higher than that in the culture of normal BM cells with GM-CSF. Thus, JMML cells, although multipotential, exhibited a predominant expansion of monocytes/macrophages in in vitro culture, compatible with the symptoms in patients with JMML, such as monocytosis and monocytic-cell infiltration to organs.

ZOL, as well as FTIs shown previously,[23] inhibited the spontaneous GM colony formation from JMML BM cells in a dose-dependent manner. It is of interest that G colonies consisting of only granulocytes, no macrophages, emerged with the addition of ZOL to the clonal culture. Because these G colonies were spontaneous colonies produced in the absence of hematopoietic factors, the spontaneous G colonies induced by the addition of ZOL seemed to originate from JMML clones, not normal hematopoietic progenitors. Cytochemical and flow cytometric analyses of the cells in the suspension culture of JMML cells also showed the decrease of mature monocytes/macrophages, but granulocytes and immature cells survived even in the presence of ZOL. Taken together, these results indicate that ZOL predominantly inhibited the differentiation of JMML cells into monocytes/macrophages but not granulocytes. This finding was confirmed in a single JMML clone, suggesting that continuously activated RAS preferentially stimulates the differentiation of JMML cells along monocyte/macrophage lineage. This notion is supported by the report that murine myeloid precursor cells with v-Ha-*Ras* were induced to differentiate along monocyte/macrophage lineage.[37]

There are at least 2 possibilities regarding the immature JMML cells that the continuously activated RAS acts on. The first one is that JMML cells already committed to the monocyte/macrophage lineage may be hastened along the pathway by the activated RAS. Second, continuously activated RAS may act on the multipotential JMML cells to commit them to differentiate into monocytes/macrophages but not other lineages, including granulocytes, because it was shown that mutational activation of RAS in murine multipotential precursor cells inhibits their differentiation into, not macrophages, but neutrophils.[38] In any case, ZOL, a RAS-blocker, arrested the JMML cells in the early stages by suppressing their differentiation into mature monocytes/macrophages.

The growth of monocytes/macrophages from normal BM cells was suppressed by 100 μM ZOL in both clonal and suspension cultures, but the effect of ZOL on granulocyte development was minor even at a higher concentration. This suggests that activated RAS also acts on immature hematopoietic cells to preferentially differentiate along monocyte/macrophage lineage in normal hematopoiesis. RAS, continuously activated in JMML cells, may accelerate their differentiation into monocytes/macrophages, although monocytes/macrophages derived from JMML cells were dysfunctional because they reacted weakly to α-NBE staining as compared with those from normal BM cells. Therefore, the massive expansion of macrophages in the culture of JMML cells may be the result of their accelerated differentiation into monocytes/macrophages. However, there remains a possibility that aberrant signaling through the RAS stimulates not only the differentiation of immature JMML cells but also the proliferation of mature monocytes/macrophages derived from immature JMML cells directly.

Aside from providing insight into molecular mechanisms behind the pathogenesis of JMML, our observation offers a novel approach to therapy in JMML because it has been proven that ZOL can be safely used in the treatment of bone disease or some cancers.[26,39] In the present study, indeed, the effect of ZOL on normal BM cells was weak as compared with that on JMML cells. Even though ZOL does not kill the immature population of JMML cells as shown by the flow cytometric analysis of the cultured JMML cells, ZOL, which prevents the massive expansion of monocytes/macrophages derived from JMML cells, could be useful for the therapy of JMML, because death in patients with JMML usually occurs as the result of monocytic-cell infiltration to organs, leading to organ dysfunction, infection, and bleeding.[1]

We mainly used the concentrations of more than 10 μM ZOL to define the difference of the effect of ZOL between JMML and normal BM cells in the present study. In the clinical situation, however, it is critical whether the serum concentration of ZOL in vivo is able to inhibit the JMML-cell growth. In the experiment using lower concentrations, ZOL had an inhibitory effect on JMML cells, although little effect on normal BM cells, even at a concentration of 3 μM, which was within the range of serum concentrations reported in a previous clinical study for the therapy of osteoporosis.[26] Although the inhibitory effect of ZOL on JMML-cell growth does not reach a maximum at such a concentration in vivo, ZOL could enhance the effectiveness of other antileukemia drugs targeting immature JMML cells in combination with such drugs.[25,40] To translate our finding to the clinical setting, further studies to clarify the molecular mechanism of the effect of ZOL and the in vivo effect of ZOL are needed.

References

1. Niemyer CM, Arico M, Basso G, et al. Chronic myelomonocytic leukemia in childhood: a report of 110 cases. Blood. 1997;89:3534-3543.
2. Emanuel PD. Myelodysplastic and myeloproliferative disorders in childhood: an update. Br J Haematol. 1999;105:852-863.
3. Arico M, Biondi A, Pui CH. Juvenile myelomonocytic leukemia. Blood. 1997;90:479-488.
4. Passmore SJ, Hann IM, Stiller CA, et al. Pediatric myelodysplasia: a study of 68 children and a new prognostic scoring systems. Blood. 1995;85:1742-1750.
5. Manabe A, Okamura J, Yumura-Yagi K, et al. Allogeneic hematopoietic stem cell transplantation for 27 children with juvenile myelomonocytic leukemia diagnosed based on the criteria of the international JMML Working Group. Leukemia. 2002; 16:645-649.
6. Lutz P, Zix-Kieffer I, Souillet G, et al. Juvenile myelomonocytic leukemia: analysis of treatment results in the EORTC children's leukemia cooperative group (CLCG). Bone Marrow Transplant. 1996;18:1111-1116.
7. Locatelli F, Nöllke P, Zecca M, et al. Hematopoietic stem cell transplantation (HSCT) in children with juvenile myelomonocytic leukemia (JMML): results of the EWOG-MDS/EBMT trial. Blood. 2005;105:410-419.
8. Emanuel PD, Bates LJ, Castleberry RP, Gualtieri RJ, Zukerman KS. Selective hypersensitivity to

granulocyte-macrophage colony-stimulating factor by juvenile chronic myeloid leukemia hematopoietic progenitors. Blood. 1991;77:925-929.
9. Suda J, Eguchi M, Akiyama Y, et al. Differentiation of blast cells from Down Syndrome patient with transient myeloproliferative disorder. Blood. 1987;69:508-512.
10. Tartaglia M, Niemyer CM, Song X, et al. Somatic PTPN11 mutations in juvenile myelomonocytic leukemia, myelodysplastic syndromes, and acute myeloid leukemia. Nat Genet. 2003;34:148-150.
11. Flotho C, Valcamonica S, Mach-Pascula S, et al. Ras mutations and clonality analysis in children with juvenile myelomonocytic leukemia (JMML). Leukemia. 1999;13:32-37.
12. Sheng XM, Kawamura M, Ohnishi H, et al. Mutations of the RAS genes in childhood acute myeloid leukemia, myelodysplastic syndrome and juvenile myelomonocytic leukemia. Leukemia Res. 1997;21:697-701.
13. Miyauchi J, Asada M, Sasaki M, et al. Mutations of the N-ras genes in juvenile chronic myelogenous leukemia. Blood. 1994;83:2248-2254.
14. Kalra R, Padermura DC, Olson K, Shannon KM. Genetic analysis is consistent with the hypothesis that NF1 limits myeloid cell growth through p21ras. Blood. 1994;84:3435-3439.
15. Side LE, Emanuel PD, Taylor B, et al. Mutations of the NF1 gene in children with juvenile myelomonocytic leukemia without clinical evidence of neurofibromatosis, type1. Blood. 1998;92:267-272.
16. Tartaglia M, Mehler EL, Goldberg R, et al. Mutations in PTPN11, encoding the protein tyrosine phosphatase SHP-2, cause Noonan syndrome. Nat Genet. 2001;29:465-468.
17. Iverson PO, Rodwell RL, Pitcher L, Taylor KM, Lopez AF. Inhibition of proliferation and induction of apoptosis in juvenile myelomonocytic leukemic cells by granulocyte-macrophage colony-stimulating factor analogue E21R. Blood. 1996;88:2634-2639.
18. Iverson PO, Lewis ID, Turczynowicz S, et al. Inhibition of granulocyte-macrophage colony-stimulating factor prevents dissemination and induces remission of juvenile myelomonocytic leukemia in engrafted immunodeficient mice. Blood. 1997;90:4910-4917.
19. Willumsen BM, Norris K, Papageorge AG, Hubbert NL, Lowy DR. Harvey murine sarcoma virus p21 ras protein: biological and biochemical significance of cysteine nearest the carboxy terminus. EMBO J. 1984;3:2581-2585.
20. Rowinski EK, Windle JJ, Von Hoff DD. Ras protein farnesyltransferase: a strategic target for anticancer therapeutic development. J Clin Oncol. 1999;17:3631-3652.
21. Jackson JH, Cochrane CG, Bourne JR, et al. Farnesol modification of Kirsten-ras exon 4B protein is essential for transformation. Proc Natl Acad U S A. 1990;87:3042-3046.
22. Peters DG, Hoover RR, Gerlach MJ, et al. Activity of farnesyl protein transferase inhibitor SCH66336 against BCR/ABL-induced murine leukemia and primary cells from patients with chronic myeloid leukemia. Blood. 2001;97:1404-1412.
23. Emanuel PD, Richard C, Wiley ST, Gopurala B, Castleberry RP. Inhibition of juvenile myelomonocytic leukemia cell growth in vitro by farnesyltransferase inhibitors. Blood. 2000;95:639-645.
24. Whyte DB, Kischmeier P, Hockenberry TN, et al. K- and N-Ras are geranylgeranylated in cells treated with farnesyl protein transferase inhibitors. J Biol Chem. 1997;272:14459-14464.
25. Jagdev SP, Coleman RE, Shipman CM, Rostami HA, Croucher PI. The bisphosphonate, zoledronic acid, induces apoptosis of breast cancer cells: evidence for synergy with paclitaxel. Br J Cancer. 2001;84:1126-1134.
26. Berenson J, Ravera C, Ma P, et al. Population pharmacokinetics of zometa [abstract]. Proc Am Soc Clin Oncol. 2002;21:209a.
27. Green JR. Chemical and biological prerequisites for novel bisphosphonate molecules: results of comparative preclinical studies. Semin Oncol. 2001;84:1126-1134.
28. Pinkel D, Aricó M, Biondi A, et al. Differentiating juvenile myelomonocytic leukemia from infectious disease [letter]. Blood. 1998;91:365-367.
29. Ebihara Y, Tsuji K, Lyman SD, et al. Synergistic action of Flt3 and gp130 signalings in human hematopoiesis. Blood. 1997;90:4363-4368.
30. Nishijima I, Nakahata T, Watanabe S, et al. Hematopoietic and lymphopoietic responses in human granulocyte-macrophage colony-stimulating factor (GM-CSF) receptor transgenic mice injected with human GM-CSF. Blood. 1997;90:1031-1038.
31. Nakahata T, Ogawa M. Hematopoietic colony-forming cells in umbilical cord blood with extensive capability to generate mono- and multipotential hematopoietic progenitors. J Clin Invest. 1982;70:1324-1328.
32. Sui X, Tsuji K, Tanaka R, et al. gp130 and c-Kit signalings synergize for ex vivo expansion of human primitive hematopoietic progenitor cells. Proc Natl Acad Sci U S A. 1995;92:2859-2863.
33. Ueda T, Tsuji K, Yoshino H, et al. Expansion of human NOD/SCID-repopulating cells by stem cell factor, Flk2/Flt3 ligand, thrombopoietin, IL-6, and soluble IL-6 receptor. J Clin Invest. 2000;105:1013-1021.
34. Tajima S, Tsuji K, Ebihara Y, et al. Analysis of interleukin 6 receptor and gp130 expressions and proliferative capability of human $CD34^+$ cells. J Exp Med. 1996;184:1357-1364.
35. Stelzer GT, Shults KE, Loken MR. CD45 gating for routine flow cytometric analysis. Use of CD45 and right-angle light scatter to gate on leukemic blasts in three-color analysis. Ann N Y Acad Sci. 1993;677:265-280.
36. Estrov Z, Grunberger T, Cahn HSL, Freedman MH. Juvenile chronic myelogenous leukemia: characterization of the disease using cell cultures. Blood. 1986;67:1382-1387.
37. Hibi S, Lohler J, Friel J, Stocking C, Ostertag W. Induction of monocytic differentiation and tumorigenicity by v-Ha-ras in differentiation-arrested hematopoietic cells. Blood. 1993;81:1841-1848.
38. Darley RL, Burnett AK. Mutant RAS inhibits neutrophil but not macrophage differentiation and allows continued growth of neutrophil precursors. Exp Hematol. 1999;27:1599-1608.
39. Chen T, Berenson J, Vescio R, et al. Pharmacokinetics and pharmacodynamics of zoledronic acid in cancer patients with bone metastases. J Clin Pharmacol. 2002;42:1228-1236.
40. Kuroda J, Kimura S, Sagawa H, et al. The third-generation bisphosphonate zoledronate synergistically augments the anti-Ph^+ leukemia activity of imatinib mesylate. Blood. 2003;102:2229-2235.

STEM CELLS AND DEVELOPMENT 14:687–696 (2005)

Original Research Report

Definitive Hematopoiesis from Acetyl LDL Incorporating Endothelial Cells in the Mouse Embryo

DAISUKE SUGIYAMA,[1–3] KEN-ICHI ARAI,[2] and KOHICHIRO TSUJI[3]

ABSTRACT

Previously, we reported generation of erythropoiesis from acetyl low-density lipoprotein (Ac-LDL)-incorporating endothelial cells (ECs) in the mouse embryo. However, it is still unclear whether the other types of definitive hematopoietic cells (HCs) can be generated from these cells. In this study, ECs at 10 days post coitum (dpc) were tagged with Ac-LDL-DiI and were shown to release DiI$^+$ HCs into the circulation after 12 h of whole embryo culture. The hematopoietic clusters in the main arteries were also stained with DiI. The circulating DiI$^+$ HCs expressed c-Kit and half of these cells displayed blastic morphology. In vitro culture and in vivo reconstitution experiments demonstrated that the circulating DiI$^+$ HCs contained definitive multipotent progenitors, including hematopoietic stem cells (HSCs). Furthermore, the sorted DiI$^+$ HCs were able to colonize the fetal liver (FL) when introduced back into the blood stream of a secondary recipient embryo. These results suggest that Ac-LDL incorporating ECs can produce definitive HSCs and HCs colonizing FL in the mouse embryo.

INTRODUCTION

In the mouse embryo, definitive hematopoiesis takes place mostly in the aortic region [para-aortic Splanchnopleura (p-Sp)/aorta-gonad-mesonephros (AGM) region], and to a lesser extent in the yolk sac (YS) (1). In the p-Sp/AGM region at 10.5 days post coitum (dpc), the hematopoietic clusters attached to the dorsal aortic floor and budding into the lumen are observed as if these clusters are born from endothelial cells (ECs) (2–4). Therefore, it has long been proposed that definitive hematopoiesis might originate from a specific subset of vascular ECs called hemogenic ECs. Several lines of evidence support the notion that hemogenic ECs were able to generate definitive HCs. VE-Cadherin$^+$/CD45$^-$ ECs isolated from the p-Sp/AGM region or YS exhibit lymphoid potential in vitro and in vivo (5,6). ECs expressing Runx1, an essential transcription factor for definitive hematopoiesis, display the potential of adult repopulating hematopoietic stem cells (HSCs) (7). The first expression of *Ly-6A*, one of the earliest genes emerging in definitive HSCs, is restricted to the cells inserted into the endothelial layer (8). Recently, we and another group reported an acetyl low-density lipoprotein (Ac-LDL)-based tracing method to follow the progeny of ECs during ontogeny in the mouse and chicken embryo (9,10). This method allows ECs to be tagged from the inside following a single intracardiac injection. Ac-LDL-DiI is specifi-

[1]Developmental Biology Laboratory, UPMC, CNRS UMR76229, 75252 Paris Cedex 05 France.
[2]Division of Molecular and Developmental Biology, Department of Basic Medical Science and [3]Division of Cellular Therapy, Advanced Clinical Research Center, The Institute of Medical Science, The University of Tokyo, Tokyo 108-8639, Japan.

cally incorporated into ECs and macrophages (9–16). The intracardiac injection was followed by whole embryo culture, and the tagged ECs were shown to generate definitive erythroid cells (10). However, it remains unclear whether these hemogenic ECs can release HSCs into the circulation. In this study, we further characterized the HCs emerging from Ac-LDL-incorporating ECs.

MATERIALS AND METHODS

Intracardiac inoculation

In all experiments except the in vivo transplantation assay, ICR mice (Nihon SLC, Japan) were used. In the in vivo transplantation assay, C57BL/6J mice (CLEA, Japan) were used as donors and Ly5.1 mice as recipients, respectively, to distinguish the donor cells. Midday was taken to be 0.5 dpc for plugged mice. Embryos at 10.0 dpc were inoculated with 0.1–0.3 μl of Ac-LDL-DiI solution (excitation, 514 nm; emission, 550 nm, Biomedical Technologies, Stoughton, MA) and those at 10.5 dpc with the labeled sorted cells by intracardiac injection as described previously (10). Briefly, embryos were isolated under the stereomicroscope (Leica MZ6, Germany) in phosphate-buffered saline (PBS). Both uterus and deciduo capsularis were removed and the YS was cut along YS arteries, with care to avoid the excessive hemorrhage. The amnion was opened so that the needle could be directed into the heart. This needle was made by pulling a glass capillary (Narishige GC-10, Japan) with a micropipette puller (Narishige, Japan). Inoculated embryos were immediately submitted to whole embryo culture within 1 h of isolation.

Whole mouse embryo culture

Inoculated and cell-injected embryos were transferred into culture bottles containing 100% rat serum supplemented with glucose 2 mg/ml in a whole embryo culture system (Ikemoto Scientific Technology, Japan) and cultured for 12 h and 4 h, respectively, at 37°C with a continuous supply of gas mixture (60% O_2 and 5% CO_2 balanced with N_2) in the dark (10). After whole embryo culture, embryos exhibiting no conspicuous bleeding and anomaly were used for further analysis.

Flow cytometry and cell sorting

Inoculated embryos were pooled and rinsed three times before blood samples were collected by bleeding. Embryos were separated into YS, AGM region, and remnants. Individual tissues were dissociated by passing through a 26-gauge needle. For surface antigen detection, cell suspensions were incubated on ice in the presence of fluorescein isothiocyanate (FITC)-conjugated anti-c-Kit, CD45.2 and Mac-1 monoclonal antibodies (mAbs), R-phycoerythrin (PE)-conjugated anti-Thy-1.2 and Gr-1, and biotin-conjugated anti-CD45.2 and B220 mAbs (all purchased from Pharmingen, San Diego, CA). When the biotin-conjugated mAb was used, cells were washed and then incubated with FITC-conjugated streptavidin (Pharmingen). Flow cytometry was performed using a FACScan (Becton Dickinson, San Jose, CA). DiI^+/c-$Kit^{+/-}$ cells were sorted from blood samples using the FACSVantage instrument (Becton Dickinson, Mountain View, CA). Sorted cells were analyzed further by assays or morphological observation.

In vitro hematopoietic culture assay

Hematopoietic progenitors were assayed using methylcellulose clonal culture consisting of 4 ml of culture medium containing 1×10^4 sorted DiI^+/c-$Kit^{+/-}$ cells, α-minimal essential medium (α = MEM; Flow Laboratories, Rockville, MD), 1.2% methylcellulose (Shinetsu Chemical, Tokyo, Japan), 30% fetal bovine serum (FBS; Hyclone Laboratories, Logan, UT), 1% deionized fraction V bovine serum albumin (Sigma Chemical Co, St. Louis, MO), and 100 μmol/L 2-mercaptoethanol (Eastman Organic Chemicals, Rochester, NY). The following cytokines were plated in 35-mm suspension culture

COLOR PLATE 1. Sections through Ac-LDL-DiI-inoculated embryos after 12 h of whole embryo culture. Sections are 7 μm thick. Original magnification, 200×. Left and right panels show phase-contrast and fluorescence microscopy, respectively. **(A)** Cross section at the level of the dorsal aorta. Arrowhead shows the hematopoietic cluster. The upper right panel shows the magnification of the hematopoietic cluster. **(B)** Cross section of umbilical artery. Arrowhead shows the hematopoietic cluster. **(C)** Cross section of omphalomesenteric artery. Arrowheads indicate the circulating DiI^+ cells.

COLOR PLATE 2. Liver colonization from endothelial cell-borne hematopoietic cells. **(A)** Fetal liver was observed under a stereomicroscope equipped with a UV laser and an appropriate filter after injection of the sorted DiI^+ cells. The illumination of DiI was observed as a yellow color. Arrows show each fetal liver lobe. **(B)** The magnified view of **A**. The DiI^+ cells with yellow color were observed in a dotted pattern inside of the fetal liver lobe. **(C,D)** Sections of **A** observed by confocal microscopy. Original magnification, 200×. The illumination of DiI was observed as a white color. Arrows show sinusoids (fetal liver blood vessels). The DiI^+ cells form small colony-like islands and colonize the extrasinusoidal regions of the fetal liver.

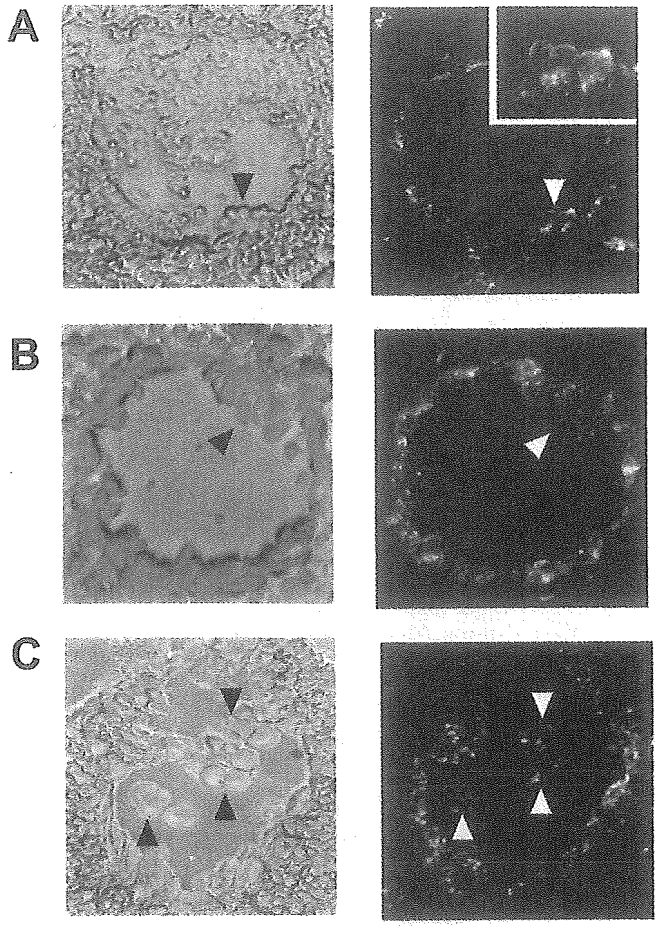

COLOR PLATE 1.

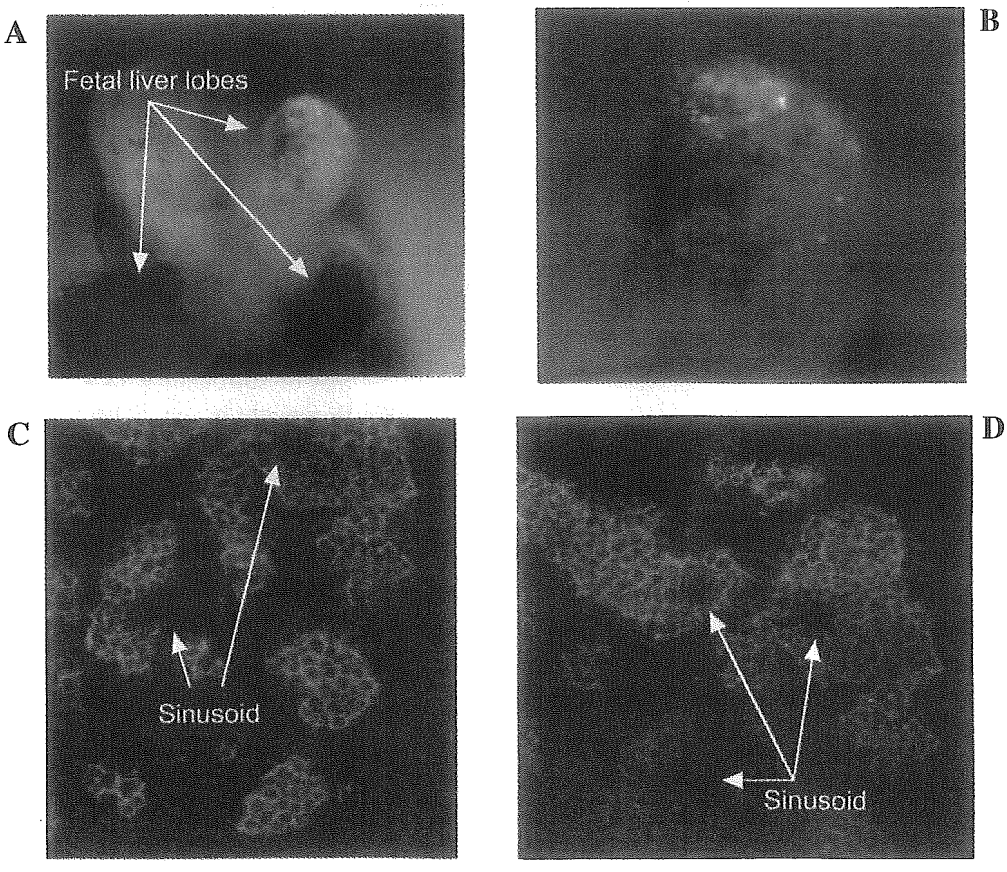

COLOR PLATE 2.

dishes (#1008, Falcon, Lincoln Park, NJ): 100 ng/ml of mouse stem cell factor (SCF) (Kirin Brewery, Japan), 10 ng/ml of mouse interleukin (IL)-3 (Kirin), 2 U/ml of human erythropoietin (EPO) (Kirin), 100 ng/ml of human IL-6 (Tosoh, Kanagawa, Japan), 20 ng/ml of human thrombopoietin (TPO) (Kirin), and 10 ng/ml human granulocyte colony-stimulating factor (G-CSF) (Kirin). The dishes were incubated at 37°C in a humidified atmosphere supplemented with 5% CO_2. Colonies were counted at day 7.

In vivo neonate transplantation assay

To examine neonatal repopulating HSCs, 10,000 labeled and sorted cells were transplanted into busulfan-treated Ly5.1 mouse neonates as described previously (17). Briefly, time-pregnant mice were injected on days 17 and 18 with 15 μg/gram busulfan (Sigma-Aldrich, St. Louis MO). The DiI$^+$ cells in blood, the AGM region, YS, and remnant tissues were sorted from the inoculated and cultured embryos by FACSVantage cell sorting (Becton Dickinson, Mountain View, CA).

The isolated cells were suspended in 25 μl of PBS and transplanted into newborn pups (at the time of delivery) using a 100-μl Hamilton syringe (Hamilton, Reno, NV). More than 1 year after transplantation, blood samples were collected and analyzed for the expression of CD45.2, Gr-1, Mac-1, B220, and Thy-1.2 by flow cytometry to confirm reconstitution of the host by donor cells.

In vivo adult transplantation assay

To examine adult repopulating HSCs, 10,000 DiI$^+$ cells sorted from the inoculated and cultured embryos were transplanted into sublethally irradiated Ly5.1 adult mice together with 1×10^5 unfractionated bone marrow cells from Ly5.1 mouse (18). More than 4 months after transplantation, blood samples were analyzed as mentioned above.

Liver hematopoietic colonization

A total of 3,000–4,000 of the sorted DiI$^+$ cells were transplanted into each embryo at 10.5 dpc by intracardiac injection, followed by whole embryo culture as described above. Four hours after whole embryo culture, fetal liver (FL) was isolated and observed under a stereomicroscope equipped with a 550-nm filter to observe the DiI illumination. Thereafter, FL tissue was fixed in 4% paraformaldehyde in PBS for 8–12 h at 4°C. Fixed embryos were hydrated with sucrose (Wako, Japan), embedded into OCT compound (cat. no. #4584, Tissue-Tek), frozen with dry ice, and sectioned at 7 μm. Sections were observed under a confocal microscope (Leica TCS SP confocal, Germany). DiI illumination was observed under the condition that excitation length was 488 nm and the detected filter was at 497–699 nm.

Cell staining

Sorted cells mentioned above and the made single cell suspension of the FL cells at 10.5 dpc were cytocentrifuged on Cytospin 2 (Shandon, Pittsburgh, PA) and stained with May-Grünwald-Giemsa (Muto Chemica, Tokyo, Japan).

RESULTS

Hematopoietic clusters stained with DiI

In our previous report, 1 h after Ac-LDL-DiI inocula tion, DiI staining was found along the entire endothelia tree. On section, DiI staining was observed in the endo thelial cell layer of the vessels. FACS analysis revealed that DiI$^+$ cells were CD31$^+$, CD34$^+$, and CD45$^-$, a antigen expression pattern characteristic for the endothe lial lineage (10). In the present study, 12 h after inocu lation, DiI staining was observed along the entire endo thelial tree under the stereomicroscope, similar to that o the 1-h timepoint reported previously (data not shown On section, DiI staining was observed in the hematopo etic clusters protruding into the aortic lumen and only few circulating cells in addition to the endothelial ce layer (Color Plate 1). At 10.5 dpc, the hematopoietic clu ters were previously shown to be present in the umbil cal artery and to a lesser degree in the omphalomese teric artery and dorsal aortic floor (3). We could find th small clusters stained with DiI in the dorsal aortic flo and relatively large ones in the umbilical artery, but n in the other arteries and veins. The illumination of A LDL-DiI can be maintained for at least 24 h in vivo a 4 days in vitro even if the tagged cells divide (9,19). T illumination of hematopoietic clusters was weaker th that of surrounding ECs (Color Plate 1). This observ tion might be due to the cell division from ECs becau the original illumination of Ac-LDL-DiI might brighter in ECs and macrophages.

Though these hematopoietic clusters seem to be or inated from ECs rather than seeded from the oth extrinsic origins and attached to ECs, there has been direct evidence showing this aspect in vivo in the ma malian embryo. On the other hand, in the avian embr it was clarified that these hematopoietic clusters ori nated from ECs incorporating Ac-LDL-DiI in vivo (The authors inoculated Ac-LDL-DiI by using intrac diac injection just before macrophages appear in circu tion (9). In this study, we inoculated mouse embryo 10.0 dpc, after macrophages appeared in the circulati

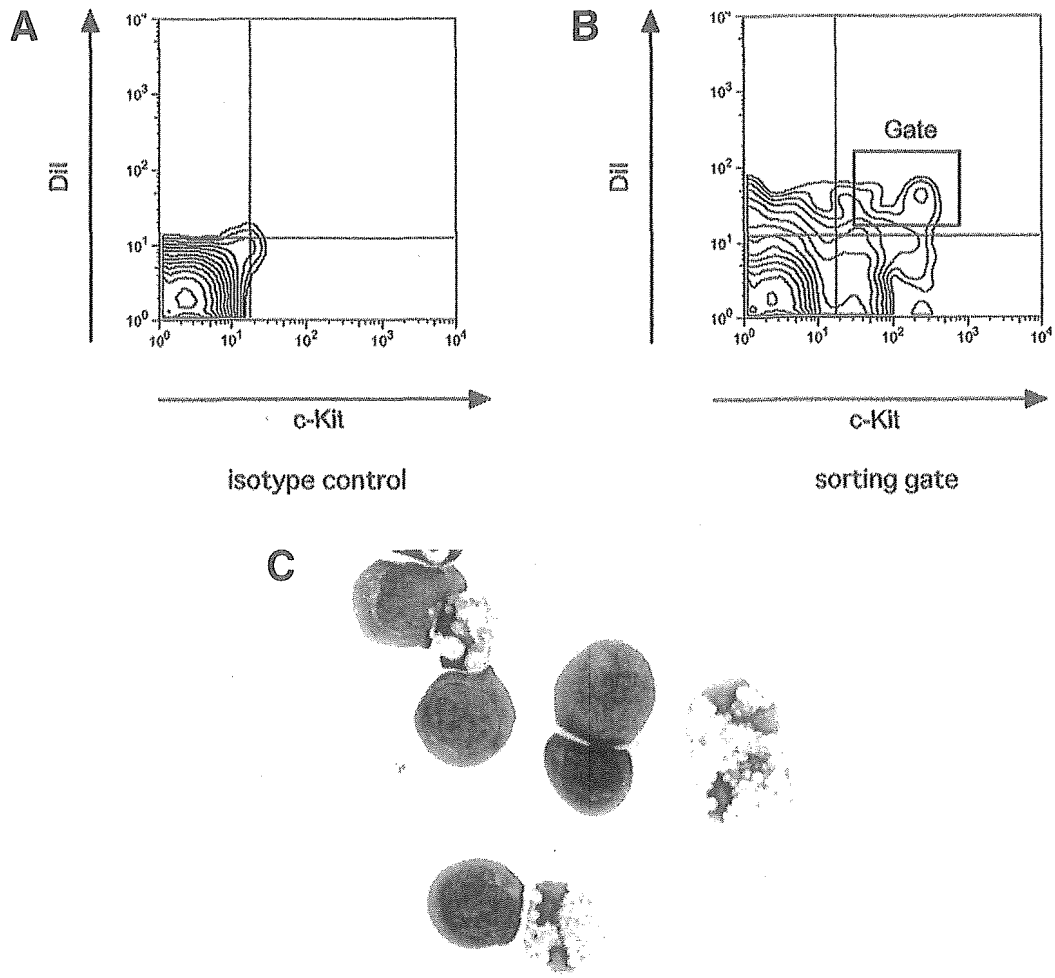

FIG. 1. The characteristics of DiI$^+$/c-Kit$^+$ cells in circulation after 12 h of inoculation. **(A,B)** The expression of c-Kit and DiI examined by flow cytometry. **(A)** Isotype control. **(B)** c-Kit and DiI expression. Gate indicates sorting gate of the DiI$^+$/c-Kit$^+$ cells. **(C)** Morphological appearance of DiI$^+$/c-Kit$^+$ cells May-Grünwald-Giemsa staining. Magnification, 400×.

which means that we could not ignore the effect of macrophages in circulation. However, it has already been reported that the phenotypic appearance of hematopoietic clusters includes expression of the antigens CD31, CD34, c-Kit, and *AML-1* in the mouse, indicating these hematopoietic clusters were immature hematopoietic progenitors or HSCs and not mature macrophages (4). In addition, in electron microscopic observations, the cells of the hematopoietic clusters are undifferentiated hemocytoblasts and are interconnected through specialized junctions exclusively of the zonula occludens type, suggesting that they are immature hematopoietic progenitors including HSCs (3). Therefore, macrophages are unlikely to comprise the hematopoietic clusters. Taken together,

TABLE 1. COLONY FORMATION OF DiI$^+$/c-KIT$^{+/-}$ CELLS

Cell fraction/ types of colony	*GM*	*Mix*	*E*	*Others*	*Total*
DiI$^+$/c-Kit$^+$	32 ± 3.6	25 ± 8	23.3 ± 0.6	37 ± 5.2	118 ± 13.5
DiI$^+$/c-Kit$^-$	1.3 ± 0.6	0	0	0	1.3 ± 0.6

The DiI$^+$/c-Kit$^{+/-}$ cells were sorted out from the blood of inoculated and cultured embryos. The number of colonies indicates the mean ± SD of triplicate cultures. Each dish contains 2,500 of the cells in 1 ml of the medium.

GM, Granulocyte/macrophage colonies; Mix, hematopoietic mixed colonies; E, erythroid bursts and erythroid/megakaryocyte colonies; Others, granulocyte colonies, macrophage colonies, and megakaryocyte colonies.

we have proposed that the hematopoietic clusters are originated from ECs tagged with Ac-LDL-DiI in vivo in the mouse embryo.

Hematopoietic potential of circulating DiI$^+$ cells in vitro and in vivo

We next examined surface markers on the circulating DiI$^+$ cells by flow cytomery. We found 15.3% of the DiI$^+$ cells expressed c-Kit, a marker for immature HCs and HSCs (Fig. 1A,B) (1,20,21). The sorted DiI$^+$/c-Kit$^+$ cells revealed two distinct populations by morphological observation—immature HCs with a blastic cell aspect and macrophages (Fig. 1C). DiI$^+$/c-Kit$^-$ cells have been reported to contain various types of immature and mature cells (10). The hematopoietic potential of DiI$^+$/c-Kit$^+$ cells was examined in methylcellulose culture assay. A total of 2,500 of the DiI$^+$/c-Kit$^+$ cells formed substantial numbers of mix-colonies, whereas 2,500 of the DiI$^+$/c-Kit$^-$ cells never displayed this activity (Table 1). DiI$^+$/c-Kit$^+$ cells could also generate both B and T lymphocytes, whereas DiI$^+$/c-Kit$^-$ cells never did, thus showing that DiI$^+$/c-Kit$^+$ cells contain definitive multipotent progenitor activity (data not shown).

We also examined in vivo reconstituting capacities of the circulating DiI$^+$ cells. It has been shown to be hard to detect HSC activity in embryonic tissues prior to 11.5 dpc when transplanting the embryonic cells into lethally irradiated adult hosts (1,17). Therefore, we first examined the DiI$^+$ cells for neonatatal repopulating HSC activity. A total of 10,000 of the DiI$^+$ cells sorted from each embryonic tissue were transplanted into conditioned neonates. The analysis of reconstituted mice were undertaken more than 1 year after transplantation. As shown in Table 2 and Fig. 2, the DiI$^+$ circulating cells contained neonatatal repopulating HSCs. Although we tried to determine which hematopoietic sites generate neonatatal repopulating HSCs, there was no significant difference in the reconstitution rate and percentage between YS and AGM regions. Remnant cells, including the circulating DiI$^+$ cells, also contained neonatatal repopulating HSCs. This result is compatible with the previous reports showing that neonatatal repopulating HSCs exist both in the YS and p-Sp/AGM region at 9 dpc and that ECs from both regions at 9.5 dpc can support hematopoiesis, suggesting that both regions are adequate microenvironments for HSCs or can generate HSCs simultaneously at this stage (17,22). In all reconstituted neonate recipients, the percentage of reconstitution was more than 80%. Such high values have also been reported previously (18,23).

In addition, experiments were extended to test the DiI$^+$ cells for adult repopulating HSC activity. One out of 7 recipients exhibited a conspicuous degree of reconstitution with a percentage of reconstitution at 13.4% (Table 2). Thus, the DiI$^+$ cells contained definitive HCs including both neonatatal and adult repopulating HSCs.

Liver colonization by circulating DiI$^+$ cells

To characterize the circulating DiI$^+$ cell behavior further, we examined whether these cells could colonize the FL via the circulation in vivo. Although some indirect experiments have suggested that the FL does not produce HCs by itself but might be colonized by HCs of extrinsic origins after 9.5 dpc, there has been no direct evidence that the FL is colonized by an extrinsic origin (24–27). The circulating DiI$^+$ cells were sorted out from the blood sample of the Ac-LDL-DiI-inoculated embryos after 12 h of WEC and showed various kinds of HCs morphologically as previously reported (9). A total of 3,000–4,000 of these sorted DiI$^+$ cells were subsequently introduced back into the circulation of a secondary re-

TABLE 2. THE RESULTS OF IN VIVO TRANSPLANTATION ASSAY

	Sorted cell population	*Reconstituted/ transplanted*
Neonate repopulating HSCs	DiI$^+$ cells in blood	3/14
	DiI$^+$ cells in AGM region	4/11
	DiI$^+$ cells in YS	3/7
	DiI$^+$ cells in remnant	2/7
Adult repopulating HSCs	DiI$^+$ cells in whole embryo	1/7

A total of 10,000 of the cells sorted from inoculated embryos were transplanted into conditioned neonates and adults, respectively. More than 1 year after transplantation, reconstitution was examined by flow cytometry. Reconstitution was defined as recipients with more than 10% of donor cells in peripheral blood. The percentage of reconstitution was calculated on the basis of the existence of donor cells expressing CD45.2 by flow cytometry.

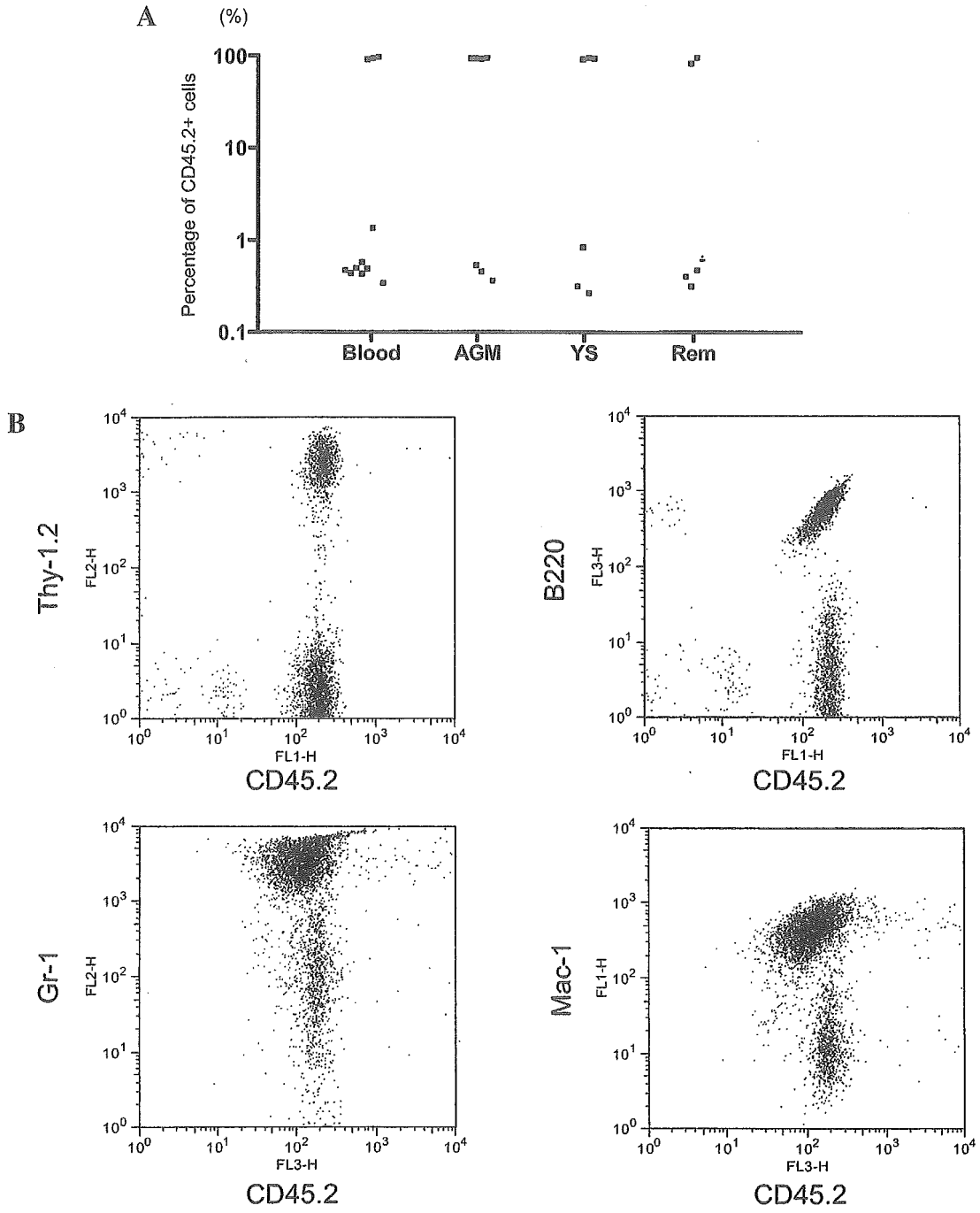

FIG. 2. Hematopoietic reconstitution by DiI$^+$ Cells. **(A)** The percentage of CD45.2$^+$ cells was analyzed in the peripheral blood of the transplanted animals by flow cytometry. Each title in the *x* axis reflects the source of the cells. Blood, AGM, YS, and Rem refer to embryonic blood, AGM region, YS, and remnant, respectively. **(B)** Fluorescence-activated cell sorting (FACS) profile of the blood, representative of the reconstituted animal.

cipient embryo at 10.5 dpc by intracardiac injection, followed by additional whole embryo culture. During this period of whole embryo culture, we can detect the illumination of DiI, as the illumination is maintained for at least 24 h, once Ac-LDL-DiI is incorporated into the cells (9). After 4 h of WEC, the FL was isolated and observed under the stereomicroscope. The DiI$^+$ cells with a yellow color were detected within the FL (Color Plate 2A,B). The rest of the DiI$^+$ cells were found in the circulation. The DiI$^+$ cells were preferentially observed in the FL lobes that did not display full erythropoiesis yet. On section, the DiI$^+$ cells were confirmed to be inside of the

FL lobe in the shape of cell aggregate, as if they formed some hematopoietic colonies, spread out, and contacted each other, or colonized in some specific regions simultaneously (Color Plate 2C,D). Relatively large-sized colonies were observed in the extrasinusoidal regions of the FL. When we injected DiI^- cells as controls, there was no DiI^+ cell-like illumination in the injected embryo, including the FL (data not shown). Thus, the circulating DiI^+ cells colonize the FL via the circulation.

Although we could show one route of EC circulation, we cannot deny there are other possibilities. In our method, it has been difficult to detect which ECs can contribute to FL colonization, but the possible candidates were likely the YS and AGM region, because both regions have already been shown to be hematopoietic sites at 9.5 dpc (1,5,6,17). We have already shown that the circulating DiI^+ cells contained various kinds of cells, including erythroid cells. It has been well known that most of the cells in the FL at this stage are erythroid cells (24–26). When we observed the morphology of the FL cells at 10.5 dpc, only 1.3 ± 0.6% (n = 3) of the cells were macrophages. Taken together, the EC-derived DiI^+ cells, especially erythroid cells, seemed to colonize the FL. Our data are in agreement with previous reports showing that the FL becomes hematopoietic beyond the 29-somite stage and that FL hematopoiesis occurs in extrasinusoidal regions (24–26). Thus, we provide evidence that ECs can generate HCs of the definitive lineage, including HSCs, into the circulation and that some of these cells can colonize the extrasinusoidal regions of the FL via the circulation in vivo in the mouse embryo.

DISCUSSION

Ac-LDL-DiI tracing method

In this study, we used the Ac-LDL-DiI tracing method as previously described (10) and followed the time course of cell activity for 16 h—12 h of WEC for Ac-LDL-DiI inoculation of the ECs and 4 h WEC for subsequent FL colonization—a time period short enough not to lose the illumination of Ac-LDL-DiI in the cells. Although the illumination of Ac-LDL-DiI might not be maintained long term, it can be maintained for at least 24 h in vivo and 4 days in vitro, even if the tagged cells divide (9,19). Once EC-borne HCs were sorted on the basis of Ac-LDL-DiI illumination, the Ly5.1 system was used as a genetic marker in the reconstitution assay to search for donor cells long-term as established by our group and others (18,21,28). Although Ac-LDL-DiI illumination would be expected to be diluted as the tagged cells divide, it remained strong and bright enough to be analyzed by a microscope equipped with fluorescence, flow cytometry, and confocal microscopy analysis.

On section, the illumination of Ac-LDL-DiI was observed in ECs, hematopoietic clusters, and circulating HCs. The illumination of hematopoietic clusters was weaker than surrounding ECs. This observation might be due to the cell division from ECs because the original illumination of Ac-LDL-DiI appeared to be bright in the ECs and circulating macrophages. After FL colonization, the DiI illumination was easily viewed with the confocal microscope. When we injected DiI^- cells from Ac-LDL-DiI-injected embryos or noninjected embryos into the recipient embryos, the illumination of DiI in the FL was never detected. This indicates that the DiI illumination was bright enough to analyze by confocal microscopy and not due to a nonspecific autofluorescence effect, and that DiI^+ cells really existed in the FL lobe. In addition, it suggests that the cells sorted out by flow cytometry on the basis of DiI illumination really possessed DiI and preserved this illumination after sorting, injection, and colonization for an additional 4 h.

Ac-LDL-DiI does not damage the cells cultured in the medium containing Ac-LDL-DiI and, thus, it is unlikely cell death was influencing the FL uptake of the labeled cells. When we sorted out the DiI^+ cells from blood samples, they appeared to be healthy HCs by morphological observation, could generate hematopoietic colonies (Table 1) and had reconstituting ability (Table 2), which means they were alive. In the FL colonization studies, the DiI^+ cells were detected as if they generated hematopoietic colonies in the FL, not randomly dispersed throughout, suggesting they acted as living progenitor cells after homing to the FL. Although this experimental strategy is limited to 24 h, it is the only method to follow up the ontogeny of ECs in the mouse embryo at the moment.

A new method using a genetic marker should be developed in the future to follow up for a longer period. Recently, it was reported that c-Kit^-/$CD45^-$ cells in the AGM region at 10.5 dpc incorporated Ac-LDL during in vitro culture, whereas only ECs and macrophages at 10.0 dpc could incorporate Ac-LDL upon intracardiac inoculation (29). Although these results might be due to the differences in labeling methods, we will need to characterize further the Ac-LDL incorporating cells when inoculating the embryos at 10.5 dpc with Ac-LDL followed by intracardiac injection.

Endothelial cell-borne hematopoietic cells in circulation

In our previous study, we showed that the circulating DiI^+ cells originated from ECs tagged with Ac-LDL-DiI (10). In this study, we demonstrated that these circulating DiI^+ cells contained multipotent definitive progenitors and HSCs. This timing of HC emergence is compatible with the previous report showing that circulating

multipotent progenitors are first detected at 10.5 dpc (30). It was already shown that CD31$^-$/VE-cadherin$^-$/Runx-1$^+$ mesenchymal cells in the AGM region also contained adult repopulating HSCs (7).

Although we cannot deny the possibility that mesenchymal cells might contribute to this hematopoietic wave, ECs can be considered to be one source of this wave. We mainly used the neonatatal transplantation assay to examine for HSC potential, because it has been shown to be hard to detect HSCs in host animals using the adult transplantation assay when we inject the embryonic tissues prior to 11.5 dpc (1). Neonatal repopulating activity in the mice transplanted with DiI$^+$ cells was achieved at more than 80%, similar to the high value of chimerism reported when other embryonic tissues have been injected into adult mouse hosts (18,23).

Although it is difficult to compare these results with others, because we analyzed the transplanted mice more than 1 year after transplantation, the high hematopoietic potential of the DiI$^+$ cells may be a result of a more complete ablation of host cells and thus a lack of competitor host cells. When adult bone marrow HSCs were transplanted into conditioned neonates, the percentage of reconstitution achieved reached 100% (31). Thus, high levels of engraftment can be attained in this model. The reason why not all the animals were completely reconstituted might be due to the technical difficulties in performing the newborn transplants and that the results represent an underestimate of the actual repopulating ability of donor cell samples.

Liver colonization from endothelial cell-borne hematopoietic cells

Circulating DiI$^+$ ECs or EC progeny colonized the FL via the circulation, consistent with the extrinsic origin of cells as hypothesized previously (24–27). Colonization was preferentially observed in the FL lobe, which did not display erythropoiesis yet, implying that the molecules for colonization were preferentially expressed in this lobe. Although there were many host cells in the circulation, some of DiI$^+$ cells could colonize FL competitively in this relatively short-term assay, suggesting that the DiI$^+$ cells could colonize the FL soon after they were released from ECs and implying that the mechanisms of FL colonization might be controlled tightly. β_1-integrin is critical in the FL colonization with hematopoietic elements, but the role of other important molecules has not been clarified (32). It will be necessary to investigate further the nature, source, and number of molecules that regulate the release of HSCs from ECs and their colonization of the FL in the near future.

ACKNOWLEDGMENTS

We thank Drs. K. Ikuta for Ly5.1 mice; A. Cumano, T. Jaffredo, N. Osumi, T. Inoue, Y. Soda, H. Yoshida, T. Yokomizo, T. Hara, and M. Ogawa for technical advice and helpful discussion; and I. Hirose, F. Ma, W. Dang, M. Wada, K. Ishikawa, Y. Fukuchi, S. Hanada, A. Takeshita, M. Satoh, and M. Itoh for technical support. This work was partially supported by the Program for Promotion of Fundamental Studies in Health Science of the Organization for Pharmaceutical Safety and Research of Japan, Sankyo Foundation of Life Science, Sumitomo Life Social Welfare Services Foundation, and Mitsukoshi Health And Welfare Foundation.

REFERENCES

1. Dzierzak E, A Medvinsky and M de Bruijn. (1998). Qualitative and quantitative aspects of hematopoietic cell development in the mammalian embryo. Immunol Today 19:228–236.
2. Wagner RC. (1980). Endothelial cell embryology and growth. Adv Microcirc 9:45–75.
3. Garcia-Porrero JA, IE Godin and F Dieterlen-Lievre. (1995). Potential intraembryonic hemogenic sites at preliver stages in the mouse. Anat Embryol 192:425–435.
4. Marshall C. (2001). The embryonic origins of human haematopoiesis. Br J Haematol 112:838–850.
5. Nishikawa SI, S Nishikawa, H Kawamoto, H Yoshida, M Kizumot, H Kataoka and Y Katsura. (1998). In vitro generation of lymphohematopoietic cells from endothelial cells purified from murine embryos. Immunity 8:761–769.
6. Fraser ST, M Ogawa, RT Yu, S Nishikawa, MC Yoder and SI Nishikawa. (2002). Definitive hematopoietic commitment within the embryonic vascular endothelial-cadherin(+) population. Exp Hematol 30:1070–1078.
7. North TE, MF de Bruijn, T Stacy, L Talebian, E Lind, C Robin, M Binder, E Dzierzak and NA Speck. (2002). Runx1 expression marks long-term repopulating hematopoietic stem cells in the midgestation mouse embryo. Immunity 16:661–672.
8. de Bruijn MF, X Ma, C Robin, K Ottersbach, MJ Sanchez and E Dzierzak. (2002). Hematopoietic stem cells localize to the endothelial cell layer in the midgestation mouse aorta. Immunity 16:673–683.
9. Jaffredo T, R Gautier, A Eichmann and F Dieterlen-Lievre. (1998). Intraaortic hemopoietic cells are derived from endothelial cells during ontogeny. Development 125:4575–4583.
10. Sugiyama D, M Ogawa, I Hirose, T Jaffredo, K Arai and K Tsuji. (2003). Erythropoiesis from Acetyl LDL incorporating endothelial cells at the pre-liver stage. Blood 101: 4733–4738.
11. Netland PA, BR Zetter, DP Via and JC Voyta. (1985). In situ labeling of vascular endothelium with fluorescent acetylated low density lipoprotein. Histochem J 17:1309–1320.

12. Pitas RE, J Boyles, RW Mahley and DM Bissell. (1985). Uptake of chemically modified low density lipoproteins in vivo is mediated by specific endothelial cells. J Cell Biol 100:103–117.
13. Brand-Saberi B, R Seifert, M Grim, J Wilting, M Kuhlewein and B Christ. (1995). Blood vessel formation in the avian limb bud involves angioblastic and angiotrophic growth. Dev Dyn 202:181–194.
14. Herz J. (2001). The LDL receptor gene family: (un)expected signal transducers in the brain. Neuron 29:571–581.
15. Kocher AA, MD Schuster, MJ Szabolcs, S Takuma, D Burkhoff, J Wang, S Homma, NM Edwards and S Itescu. (2001). Neovascularization of ischemic myocardium by human bone-marrow-derived angioblasts prevents cardiomyocyte apoptosis, reduces remodeling and improves cardiac function. Nature Med 7:430–436.
16. Wu S, J Sangerman, M Li, GH Brough, SR Goodman and T Stevens. (2001). Essential control of an endothelial cell ISOC by the spectrin membrane skeleton. J Cell Biol 154:1225–1233.
17. Yoder MC, K Hiatt, P Dutt, P Mukherjee, D-M Bodine and D Orlic. (1997). Characterization of definitive lymphohematopoietic stem cells in the day 9 murine yolk sac. Immunity 7:335–344.
18. Matsuoka S, K Tsuji, H Hisakawa, MJ Xu, Y Ebihara, T Ishii, D Sugiyama, A Manabe, R Tanaka, Y Ikeda, S Asano and T Nakahata. (2001). Generation of definitive hematopoietic stem cells from murine early yolk sac and paraaortic splanchnopleures by aorta-gonad-mesonephros region-derived stromal cells. Blood 98:6–12.
19. Hara T, Y Nakano, M Tanaka, K Tamura, T Sekiguchi, K Minehata, NG Copeland, NA Jenkins, M Okabe, H Kogo, Y Mukouyama and A Miyajima. (1999). Identification of Podocalyxin-like protein 1 as a novel cell surface marker for hemangioblasts in the murine Aorta-Gonad-Mesonephros region. Immunity 11:567–578.
20. Ogawa M, Y Matsuzaki, S Nishikawa, S Hayashi, T Kunisada, T Sudo, T Kina, H Nakauchi and S Nishikawa. (1991). Expression and function of c-kit in hemopoietic progenitor cells. J Exp Med 174:63–71.
21. Sanchez MJ, A Holmes, C Miles and E Dzierzak. (1996). Characterization of the first definitive hematopoietic stem cells in the AGM and liver of the mouse embryo. Immunity 5:513–525.
22. Li W, SA Johnson, WC Shelley, M Ferkowicz, P Morrison, Y Li and MC Yoder. (2003). Primary endothelial cells isolated from the yolk sac and para-aortic splanchnopleura (P-Sp) support the expansion of adult marrow stem cells in vitro. Blood 102:4345–4353.
23. Gekas C, F Dieterlen-Lievre, SH Orkin and HK Mikkola. (2005). The placenta is a niche for hematopoietic stem cells. Dev Cell 8:365–375.
24. Johnson GR and RO Jones. (1973). Differentiation of the mammalian hepatic primordium in vitro. I. Morphogenesis and the onset of haematopoiesis. J Embryol Exp Morphol 30:83–96.
25. Johnson GR and MA Moore. (1975). Role of stem cell migration in the initiation of mouse foetal liver haemopoiesis. Nature 258:726–728.
26. Houssaint E. (1981). Differentiation of the mouse hepatic primordium. II. Extrinsic origin of the haemopoietic cell line. Cell Differ 10:243–252.
27. Cudennec CA, JP Thiery and N Le Douarin. (1981). In vitro induction of adult erythropoiesis in early mouse yolk sac. Proc Natl Acad Sci USA 78:2412–2416.
28. Cumano A, JC Ferraz, M Klaine, JP Di Santo and I. Godin. (2001). Intraembryonic, but not yolk sac hematopoietic precursors, isolated before circulation, provide long-term multilineage reconstitution. Immunity 15:477–485.
29. Bertrand JY, S Giroux, R Golub, M Klaine, A Jalil, L Boucontet, I Godin and A Cumano. (2005). Characterization of purified intraembryonic hematopoietic stem cells as a tool to define their site of origin. Proc Natl Acad Sci USA 102:134–139.
30. Delassus S and A Cumano. (1996). Circulation of hematopoietic progenitors in the mouse embryo. Immunity 4:97–106.
31. Yoder MC, JG Cumming, K Hiatt, P Mukherjee and DA Williams. (1996). A novel method of myeloablation to enhance engraftment of adult bone marrow cells in newborn mice. Biol Blood Marrow Transplant 2:59–67.
32. Hirsch E, A Iglesias, AJ Potocnik, U Hartmann and R. Fassler. (1996). Impaired migration but not differentiation of haematopoietic stem cells in the absence of beta-1 integrins. Nature 380:171–175.

Address reprint requests to:
Dr. Daisuke Sugiyama
Department of Biochemistry
Dartmouth Medical School
7200 Vail Building
Hanover, NH 03755

E-mail: ds-mons@yb3.so-net.ne.jp

Dr. Kohichiro Tsuji
Division of Cellular Therapy
IMSUT
Tokyo 108-8639 Japan

Received March 23, 2005; accepted June 17, 2005.

bjh research paper

Methylation status of the *p15* and *p16* genes in paediatric myelodysplastic syndrome and juvenile myelomonocytic leukaemia

Daisuke Hasegawa[1,2], Atsushi Manabe[1,3], Takeo Kubota[4,5], Hirohide Kawasaki,[1] Imiko Hirose,[1] Yoshitoshi Ohtsuka,[1] Toshihisa Tsuruta,[1] Yasuhiro Ebihara,[1] Yu-ichi Goto,[4] Xiao Yan Zhao,[6] Kazuo Sakashita,[6] Kenichi Koike,[6] Mariko Isomura,[7] Seiji Kojima,[7] Akinori Hoshika,[2] Kohichiro Tsuji[1] and Tatsutoshi Nakahata[8]

[1]Department of Paediatric Haematology-Oncology, Institute of Medical Science, University of Tokyo, Tokyo, [2]Department of Paediatrics, Tokyo Medical University, Tokyo, [3]Department of Paediatrics, St Luke's International Hospital, Tokyo, [4]Department of Mental Retardation and Birth Defect Research, National Institute of Neuroscience, National Centre of Neurology and Psychiatry, Tokyo, [5]Department of Epigenetic Medicine, Faculty of Medicine, Interdisciplinary Graduate School of Medicine and Engineering, University of Yamanashi, Yamanashi, [6]Department of Paediatrics, Shinshu University School of Medicine, Matsumoto, [7]Department of Developmental Paediatrics, Nagoya University, School of Medicine, Nagoya, and [8]Department of Paediatrics, Kyoto University, School of Medicine, Kyoto, Japan

Received 29 September 2004; accepted for publication 20 December 2004

Correspondence: Atsushi Manabe, MD, Department of Paediatrics, St Luke's International Hospital, 9-1, Akashicho, Chuo-ku, Tokyo 104-8560, Japan.
E-mail: manabe-luke@umin.ac.jp

Summary

Aberrant DNA methylation is frequently observed in adults with myelodysplastic syndrome (MDS), and is recognized as a critical event in the disease's pathogenesis and progression. This is the first report to investigate the methylation status of *p15* and *p16*, cell cycle regulatory genes, in children with MDS ($n = 9$) and juvenile myelomonocytic leukaemia (JMML; $n = 18$) by using a methylation-specific polymerase chain reaction. The frequency of *p15* hypermethylation in paediatric MDS was 78% (7/9), which was comparable to that in adult MDS. In contrast, *p15* hypermethylation in JMML was a rare event (17%; 3/18). In JMML, clinical and laboratory characteristics including *PTPN11* mutations and aberrant colony formation were not different between the three patients with hypermethylated *p15* and the others. Aberrant methylation of *p16* was not detected in children with either MDS or JMML. Since *p15* and *p16* genes were unmethylated in two children with JMML, in whom the disease had progressed with an increased number of blasts, a condition referred to as blastic crisis, we infer that the aberrant methylation of these genes is not responsible for the progression of JMML. The results suggest that demethylating agents may be effective in most children with MDS and a few patients with JMML.

Keywords: myelodysplastic syndrome, juvenile myelomonocytic leukaemia, childhood, p15, aberrant methylation.

Myelodysplastic syndrome (MDS) occurs predominantly in the elderly but rarely in childhood, and a substantial difference exists between MDS in adults and in children (Sasaki *et al*, 2001; Hasle *et al*, 2003). Juvenile myelomonocytic leukaemia (JMML), categorized as a disorder bridging MDS with myeloproliferative diseases (MPD) by the World Health Organization (WHO) (Emanuel, 1999; Vardiman *et al*, 2001), is a unique disease that only occurs in childhood (Arico *et al*, 1997; Niemeyer *et al*, 1997). Mutations in the *PTPN11* gene, which is the main gene responsible for Noonan syndrome and known to be involved in the Ras/mitogen-activated protein kinase (MAPK) pathway, have recently been detected in 30–40% of patients with JMML and were thought to contribute to the pathogenesis in a subset of these patients (Isomura *et al*, 2003; Tartaglia *et al*, 2003; Loh *et al*, 2004).

  doi:10.1111/j.1365-2141.2005.05392.x

Recently, epigenetic alterations, such as the aberrant methylation of CpG islands in the promoter regions of genes, have been reported to inactivate tumour-suppressor genes and to contribute to tumorigenesis (Jones & Laird, 1999), and many genes were found to be silenced by methylation in solid tumours and haematological malignancies (Herman & Baylin, 2003). p15/INK4B and p16/INK4A, members of a family of cyclin-dependent kinase (CDK) inhibitors, are critically involved in the regulation of the cell cycle and recognized as tumour suppressors. In addition, *p15* has been recently suggested to act as a regulator of proliferation and differentiation in myelo-monocytic and megakaryocytic lineages by arresting the cell cycle (Teofili *et al*, 1998, 2000, 2001; Sakashita *et al*, 2001). Therefore, the silencing of these genes via aberrant methylation is a critical event in leukaemogenesis. In fact, methylation of the *p15* gene has frequently been demonstrated in acute leukaemia, both in adults and in children (Herman *et al*, 1997; Guo *et al*, 2000; Wong *et al*, 2000; Toyota *et al*, 2001; Garcia-Manero *et al*, 2002, 2003; Gutierrez *et al*, 2003). In contrast, *p16* is rarely methylated in haematological malignancies (Herman *et al*, 1997; Guo *et al*, 2000; Wong *et al*, 2000; Toyota *et al*, 2001; Garcia-Manero *et al*, 2002, 2003; Gutierrez *et al*, 2003).

In MDS, the aberrant methylation of *p15* correlated with morphological subtypes; it occurred frequently in those with blast expansion, such as refractory anaemia with excess blasts (RAEB), RAEB in transformation (RAEBt) and acute myeloid leukaemia (AML) evolving from MDS, whereas it occurred rarely in those with refractory anaemia (RA) and RA with ringed sideroblast (RARS) (Uchida *et al*, 1997; Quesnel *et al*, 1998; Daskalakis *et al*, 2002; Aoki *et al*, 2003). In chronic myelomonocytic leukaemia (CMML), another disorder belonging to MDS/MPD, the frequency of *p15* hypermethylation was intermediate (Uchida *et al*, 1997; Quesnel *et al*, 1998; Daskalakis *et al*, 2002; Aoki *et al*, 2003; Tessema *et al*, 2003). These studies reported the methylation status only in adult patients with MDS and MPD. No reports have examined the methylation status of cell cycle regulatory genes in childhood MDS and MPD. Here, we report the frequency of aberrant methylation of the *p15* and *p16* genes in paediatric MDS and JMML.

Patients and methods

Patients

Children suspected of having MDS or JMML were enrolled on the prospective diagnostic register of the MDS committee of the Japanese Society of Paediatric Haematology. The diagnosis was verified by the pathological review board of the committee (Manabe & Nakahata, 2003). Bone marrow (BM) or peripheral blood (PB) samples were obtained prior to treatment from patients with MDS or JMML, and sent to the Institute of Medical Science, University of Tokyo. Informed consent was obtained from the guardians of the patients following institutional guidelines. In total, samples from 27 children were analysed. The final diagnosis was refractory cytopenia with multilineage dysplasia (RCMD) in one subject, RAEB in two, CMML in two, and JMML in 18, including two children who were diagnosed with AML that had transformed from JMML. It was difficult to differentiate RAEB from AML-M6 in four children, and such cases were categorized as RAEB/M6 (Manabe & Nakahata, 2003; Manabe *et al*, 2003). In this study, there were no cases of MDS/JMML occurring secondary to a previous chemotherapy or immunosuppressive therapy, or to a constitutional abnormality, such as Noonan syndrome, neurofibromatosis-1 or Down syndrome (Hasle *et al*, 2003). The diagnosis was made according to the French–American–British (FAB) and WHO classification, and patients with JMML were diagnosed based on the diagnostic criteria proposed by the International JMML Working Group (Niemeyer *et al*, 1998). The characteristics of patients analysed in this study are listed in Tables I and II. In addition, we analysed samples from normal adult volunteers (PB; $n = 3$, BM; $n = 1$).

Table I. Clinical and laboratory characteristics of patients with MDS other than JMML.

UPN	Age (years) at presentation	Gender	Sample	Subtype	BM blast (%)	WBC ($\times 10^9$/l)	Karyotype	*PTPN11* mutation	Hypermethylation *p15*	Hypermethylation *p16*
M1	14	M	BM	RCMD	1·6	2·6	−7	GC	+	−
M2	17	M	BM	RAEB	1·6	9·2	Normal	GC	−	−
M3	13	F	BM	RAEB	13·0	4·0	Normal	Not tested	−	−
M4	9 Months	F	BM	RAEB/M6	1·3	7·1	Normal	GC	+	−
M5	12	M	PB	RAEB/M6	20·8	1·9	Normal	GC	+	−
M6	14	M	BM	RAEB/M6	0·6	1·2	Normal	GC	+	−
M7	4	F	BM	RAEB/M6	6·0	2·8	Normal	GC	+	−
M8	12	M	PB	CMML	14·0	38·6	Normal	GC	+	−
M9	17	F	BM	CMML	10·0	3·1	Add (12), inv (5)	GC	+	−

BM, bone marrow; PB, peripheral blood; RCMD, refractory cytopenia with multilineage dysplasia; RAEB, refractory anaemia with excess blasts; CMML, chronic myelomonocytic leukaemia; GC, germline configuration.

Table II. Clinical and laboratory characteristics of patients with JMML.

UPN	Age (months)/gender	Sample	BM blast (%)	WBC (10^9/l)	PB monocyte (10^9/l)	Karyotype	*PTPN11* mutation	Aberrant colony	Hypermethylation *p15*	Hypermethylation *p16*
J1	3/F	PB	1·0	36·5	1·5	Normal	GC	+	–	–
J2	14/M	PB	7·0	28·4	8·0	Normal	GC	–	–	–
J3	4/M	BM	1·0	72·3	19·5	Normal	GC	+	–	–
J4	4/F	BM	6·0	37·3	2·2	Normal	215C>T	+	–	–
J5	7/F	BM	0·4	8·3	1·3	Normal	GC	+	–	–
J6	32/M	BM	10·0	64·1	7·1	Normal	GC	+	–	–
J7	35/F	BM	6·9	43·1	5·2	Normal	179G>T	+	–	–
J8	54/M	BM	8·4	15·9	2·1	Normal	226G>A	+	–	–
J9	69/M	BM	8·2	7·6	4·6	−7	GC	+	–	–
J10	63/M	BM	1·6	26·6	3·2	Normal	179G>T	+	+	–
J11	1/M	PB	7·3	151·0	46·8	−7	GC	+	+	–
J12	37/F	PB	1·0	16·2	3·2	Normal	226G>A	+	–	–
J13	50/M	PB	2·8	16·7	3·3	Normal	GC	–	+	–
J14	6/M	BM	7·0	15·0	4·4	10p+	n.t.	+	–	–
J15	39/F	BM	1·5	27·6	4·1	Normal	n.t.	+	–	–
J16	61/F	BM	3·8	70·7	14·8	Normal	n.t.	+	–	–
J17*	35/F	BM	3·2	41·9	7·1	Normal	226G>A	+	–	–
J18*	36/M	BM	not estimated†	4·1	0·8	t (11;13)	155C>G 227A>C	–	–	–

*J17 and J18 were diagnosed with AML that had evolved from JMML. Samples were obtained at the time of diagnosis of AML.
†BM could not be estimated because of fibrosis.

Methylation-specific polymerase chain reaction

The method of bisulphite treatment and methylation-specific polymerase chain reaction (MSP) was previously described (Kubota *et al*, 1997). Briefly, mononuclear cells (MNC) were isolated by density gradient centrifugation on Ficoll-Paque (Amersham Biosciences, Piscataway, NJ, USA) from BM and PB, and genomic DNA was extracted with a QIAamp DNA Blood Midi Kit (Qiagen, Hilden, Germany). The DNA (1 μg) was first denatured by 0·2 mol/l NaOH for 10 min at 37°C, and incubated at 55°C for 16–22 h with 0·5 mmol/l hydroquinone (Sigma-Aldrich, St Louis, MO, USA) and 3·1 mol/l sodium hydrogensulphite (Sigma-Aldrich). The modified DNA was purified using the Wizard DNA Clean-Up System (Promega, Madison, WI, USA) with a Vac-Man Laboratory Vacuum Manifold (Promega). Modification was completed by desulphonation with 0·3 mol/l NaOH for 5 min at room temperature, followed by ethanol precipitation. The DNA was resuspended in Tris-EDTA.

Primers used for the methylation analysis of *p15* and *p16* are shown in Table III (Herman *et al*, 1996). Each polymerase chain reaction (PCR) was carried out in a 20 μl volume containing 19 μl of Platinum PCR superMix (a mixture of anti-Taq DNA polymerase antibody, Mg, deoxyribonucleotide triphosphates, and recombinant Taq DNA polymerase; Invitrogen, CA, USA) and 1 μl of bisulphite-modified DNA (~20 ng). PCR conditions were as follows: 95°C for 10 min, then 35 cycles at 94°C for 30 s, 60°C for 30 s, 72°C for 30 s, and a final extension of 10 min at 72°C. PCR products were loaded on 1·5% agarose gels, stained with ethidium bromide and visualized under ultra violet illumination. DNA extracted from PB of healthy donors was used as a control, and universally methylated DNA (CpGenome Universal Methylated DNA; Serologicals Corporation, Norcross, GA, USA) was used as a methylated control in all analyses.

Table III. Primer sequences* for methylation-specific PCR.

Primer set	Primer sequence (5′ – 3′)
p15-Mf	GCGTTCGTATTTTGCGGTT
p15-Mr	CGTACAATAACCGAACGACCGA
p15-Uf	TGTGATGTGTTTGTATTTTGTGGTT
p15-Ur	CCATACAATAACCAAACAACCAA
p16-Mf	TTATTAGAGGGTGGGGCGGATCGC
p16-Mr	GACCCCGAACCGCGACCGTAA
p16-Uf	TTATTAGAGGGTGGGGTGGATTGT
p16-Ur	CAACCCCAAACCACAACCATAA

M, methylated allele-specific primer; U, unmethylated allele-specific primer; f, forward; r, reverse.
*Herman *et al* (1996).

Quantitative reverse transcription-polymerase chain reaction (RT-PCR) analysis

The quantification of mRNA levels was performed with a real time fluorescence detection method according to the procedure described previously (Shimizu *et al*, 2003; Tsuzaka *et al*,

2003). To obtain the template for standards, total RNA was isolated from normal BM MNC using Isogen (Wako, Osaka, Japan), based on the evidence that normal marrow cells expressed *p15* (Sakashita *et al*, 2001). Total RNA was extracted from MNC using an RNeasy kit (Qiagen), following the manufacturer's instructions. cDNA was prepared using an RNA PCR kit (AMV) version 2.1 (Takara Shuzo, Ohtsu, Japan). The specific primer pair and probe were designed with the aid of the Primer Express program (Applied Biosystems, Foster City, CA). A target DNA fragment was amplified by PCR, fused into a pGEM-T Vector (Promega Corp.), amplified, and refined. A standard curve was constructed with serial dilution (10–10^6) of a plasmid, each containing a cDNA insert of human *p15* or *glyceraldehyde 3-phosphate dehydrogenase* (*GAPDH*) gene. Real-time PCR was performed in an ABI PRISM 7700 Sequence Detection System (Applied Biosystems), using primer pair and an oligonucleotide probe with a 5′ fluorescent reporter dye (6-carboxyfluorescein; 6FAM) and a 3′ quencher dye (carboxytetramethylrhodamine; TAMRA).

In each experiment, duplicates of a standard dilution series of specific plasmids containing cDNA from normal marrow cells and 25 ng of cDNA of unknown samples were amplified in a 50 μl reaction containing 1X Universal PCR Master Mix (Applied Biosystems), 900 nmol/l of primer pair, 200 nmol/l of an oligonucleotide probe with a 5′ fluorescent reporter dye and a 3′ quencher dye. Relative gene expression was determined based on the threshold cycles of the gene for *p15* or *GAPDH*. The assays were performed in triplicate, and mean values of the three experiments were given. The RNA of MO7e (*p15* is methylated) and ku812 (*p15* is unmethylated) were used as a negative control and a positive control respectively.

The primer and probe sequences are as follows: (1) *p15*, 5′-ATCCCAACGGAGTCAACCG-3′, 6FAM 5′-TTCGGGAGGCGCGCGATCC-3′ TAMRA, and 5′-GCTGCCCATCATCATGACC-3′; (2) *GAPDH*, 5′-GAAGGTGAAGGTCGGAGT-3′, 6FAM 5′-CAAGCTTCCCGTTCTCAGCC-3′ TAMRA, 5′-AAGATGGTGATGGGATTTC-3′.

Detection of PTPN11 mutations

Exon 3 and exon 8 of *PTPN11* including the exon–intron boundary were amplified by PCR using previously described primer pairs (Kosaki *et al*, 2002). A total of 100 ng of genomic DNA was amplified in a 25 μl reaction buffer containing 0·3 pmol/μl of each primer, 0·2 mmol/l of deoxynucleotide triphosphate, 1·0 mmol/l of $MgCl_2$ and 0·5 U of KOD-Plus-DNA Polymerase (Toyobo, Osaka, Japan). The amplification was carried out in a thermalcycler (GeneAmp PCR System 9700; Applied Biosystems) with an initial denaturation step (2 min, 94°C), followed by 35 cycles consisting of three steps: 15 s at 94°C, 30 s at 58°C and 1 min at 68°C, and an extension step (8 min, 68°C). The amplified products were analysed using 2% agarose gel electrophoresis and purified with a QIAquick PCR Purification Kit (Qiagen). The products were then cloned into the pGEM-T Easy Vector System (Promega). Eight recombinant colonies were removed and plasmid DNA was extracted using a QIAprep spin plasmid miniprep kit (Qiagen). Both sense and anti-sense strands were sequenced using the ABI BigDye Terminator v3·1 Cycle Sequencing Kit (Applied Biosystems) with T7 and SP6 Promoter primers (Promega) by automatic DNA sequencer (ABI Prism 3100 Genetic Analyzer). Using the cDNA sequence of the human *PTPN11* gene (GenBank accession no. NM002834) as the query, a homology search of the GenBank database was performed with the Basic Local Alignment Search Tool 2 (BLAST2) program.

The in vitro colony assay

In order to aid in the diagnosis of JMML (Niemeyer *et al*, 1998), MNC from PB or BM of patients suspected of having JMML were subjected to a methylcellulose colony assay as reported previously (Ebihara *et al*, 2002). Briefly, 1 ml aliquots of culture mixture containing 2×10^4 MNC, alpha-medium, 0·9% methylcellulose, 30% fetal bovine serum (FBS), 1% bovine serum albumin (BSA) and 5×10^{-5} mol/l 2-mercaptoethanol were plated in standard 35 mm non-tissue culture dishes. To each mixture was added granulocyte-macrophage colony-stimulating factor (GM-CSF), whose concentration ranged from 0 to 10 ng/ml. Cultures were performed in duplicate, and the number of colonies consisting of more than 40 cells was scored after 14 d of incubation at 37°C in a humidified atmosphere with 5% CO_2. Aberrant colony formation was defined as the spontaneous formation of colonies or hypersensitivity to GM-CSF (Emanuel *et al*, 1991).

Results

Methylation status of p15 and p16 in children with MDS other than JMML

We analysed the methylation status of cell cycle regulatory genes, *p15* and *p16*, in children with MDS other than JMML. Aberrant methylation of *p15* was detected in seven of nine children (78%) whereas none of the patients demonstrated hypermethylation of *p16* (Table I). A representative MSP result is shown in Fig 1. Both *p15* and *p16* were found to be unmethylated in all samples from the normal adult volunteers.

Methylation status of p15 and p16 in children with JMML

In children with JMML, the hypermethylation of *p15* was detected in only three of 18 cases (17%; Fig 1, Table II). The gene was unmethylated in patients with AML occurring after JMML (cases J17 and J18) as well (Table II). Aberrant methylation of *p16* was undetectable in all patients with JMML. The clinical and laboratory characteristics including karyotype, colony growth *in vitro* and mutations in *PTPN11* did not differ between the three patients (cases J10, J11 and J13) with hypermethylated *p15* and the others (Table IV).

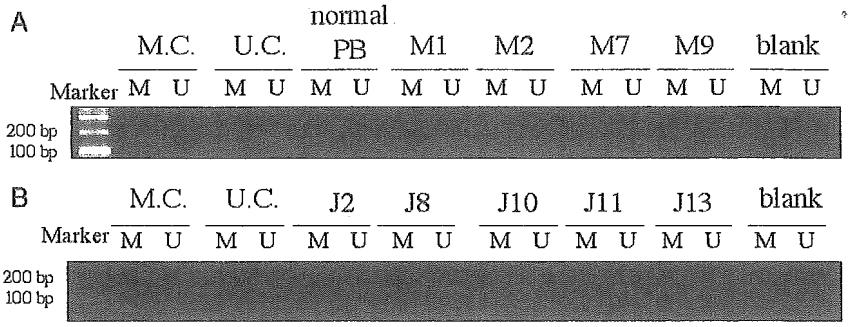

Fig 1. Methylation specific PCR for the *p15* gene in paediatric MDS (a) and JMML (b). M = methylated allele; and U = unmethylated allele. Universally methylated DNA and DNA extracted from PB of normal adult volunteers was used as a methylated control (M.C.) and unmethylated control (U.C.) in all analyses respectively. PCR without a DNA template (blank) was performed in all analyses as well.

Table IV. Comparison of clinical and laboratory characteristics of three patients with JMML and *p15* hypermethylation and those without *p15* hypermethylation.

	J10	J11	J13	Other cases (n = 15), median (range)
Age at presentation (months)	63	1	50	34 (3–69)
Gender	Male	Male	Male	Male:female = 7:8
WBC ($\times 10^9$/l)	26·6	151·0	16·7	28·4 (4·1–72·3)
Monocytes ($\times 10^9$/l)	3·2	46·8	3·3	4·5 (0·8–19·5)
Hb (g/dl)	11·9	8·4	7·6	9·5 (6·3–12·5)
Platelets ($\times 10^9$/l)	54·0	34·0	267·0	38·0 (7·0–171·0)
HbF (%)	23·0	Not tested	16·0	26·5 (1·0–78·0)
BM nucleated cells ($\times 10^9$/l)	384·0	235·0	241·0	329·0 (72·0–840·0)
Blasts in BM (%)	1·6	7·3	2·8	4·9 (0·4–10·0)
Monocytes in BM (%)	4·4	4·3	5·7	4·9 (0·4–14·8)
Aberrant colony formation	(+)	(+)	(−)	(+) in 13 of 15 cases
PTPN11 mutation	(+)	(−)	(−)	(+) in 6 of 12 tested
Karyotype	Normal	−7	Normal	Abnormal in three of 15 cases

Expression of p15 mRNA in children with MDS and JMML

We performed a real-time quantitative RT-PCR to assess the correlation between hypermethylation and expression of the *p15* gene in 10 patients whose RNA was available (methylated *p15*; n = 5, unmethylated *p15*; n = 5). We did not find a significant difference in *p15* expression level between the subgroup with *p15* methylation and the subgroup without *p15* methylation (Mann–Whitney test); the mean expression level of *p15* normalized by the expression level of *GAPDH* was $3{\cdot}01 \times 10^{-4}$ and $3{\cdot}43 \times 10^{-4}$ respectively (Fig 2). The expression level in MO7e (negative control) was $0{\cdot}14 \times 10^{-4}$, whereas that in ku812 (positive control) was $5{\cdot}71 \times 10^{-4}$.

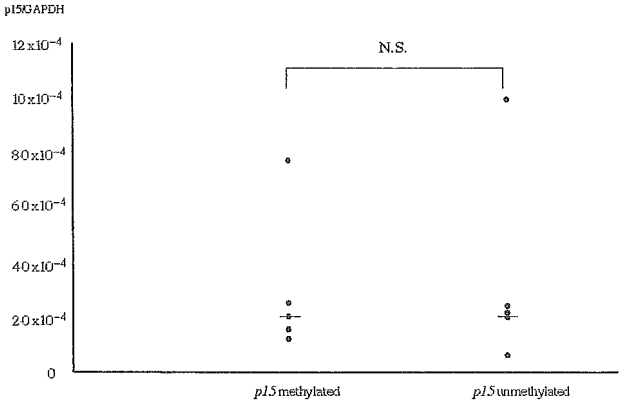

Fig 2. *p15* mRNA levels were measured by quantitative, real-time RT-PCR. The expression levels are displayed as ratios between *p15* and *GAPDH*. The horizontal bar indicates the median value of each group. The expression level of *p15* in the subgroup with *p15* methylation (n = 5) was not different from that in the subgroup without *p15* methylation (n = 5; Mann–Whitney test).

PTPN11 mutation in paediatric MDS and JMML

We detected *PTPN11* mutations in seven of 15 children with JMML (47%; Table II). In contrast, eight children with MDS other than JMML were found to have the germline configuration in *PTPN11* (Table I). No children with JMML or MDS in this study had been diagnosed with Noonan syndrome or neurofibromatosis-1.

In vitro colony assay in JMML

We performed an *in vitro* colony assay in all 18 patients with JMML. Of those, the spontaneous formation of colonies or hypersensitivity to GM-CSF was demonstrated in 15 cases (Table II).

Discussion

The aberrant methylation of tumour-suppressor genes is now recognized as a well-established event in the development and

progression of solid tumours and haematological malignancies (Jones & Laird, 1999; Herman & Baylin, 2003). Several studies have reported that the *p15* gene, encoding a CDK inhibitor, is frequently methylated in adult patients with acute leukaemia and MDS (Herman *et al*, 1997; Uchida *et al*, 1997; Quesnel *et al*, 1998; Cameron *et al*, 1999; Guo *et al*, 2000; Wong *et al*, 2000; Toyota *et al*, 2001; Daskalakis *et al*, 2002; Garcia-Manero *et al*, 2002, 2003; Aoki *et al*, 2003; Gutierrez *et al*, 2003; Tessema *et al*, 2003). In paediatric patients with acute lymphoblastic leukaemia (ALL) and AML, *p15* was methylated as frequently as in adult patients (Herman *et al*, 1997; Guo *et al*, 2000; Wong *et al*, 2000; Garcia-Manero *et al*, 2003; Gutierrez *et al*, 2003). To our knowledge, there have been no reports investigating the methylation status of cell cycle regulatory genes in paediatric MDS and MPD.

In this study, we examined the methylation status of the *p15* and *p16* genes in nine children with MDS other than JMML and 18 children with JMML using MSP, a reliable method of detecting methylated alleles (Herman *et al*, 1996). The frequency of *p15* hypermethylation in paediatric MDS other than JMML was 78%, which was comparable with that in adult MDS. In contrast, we found that the frequency of *p15* hypermethylation was much lower in patients with JMML (3/18; 17%) than adults with each subtype of MDS or with CMML (Uchida *et al*, 1997; Quesnel *et al*, 1998; Daskalakis *et al*, 2002; Aoki *et al*, 2003; Tessema *et al*, 2003). The clinical and laboratory characteristics of the three patients with *p15* hypermethylation were not different from those of the others. It is known that a deregulated Ras signalling pathway, including neurofibromin encoded by *NF-1* and SHP-2 encoded by *PTPN11*, is responsible for the leukaemogenesis in a majority of patients with JMML and that mutations in *Ras*, *NF1* and *PTPN11* are mutually exclusive in JMML (Miyauchi *et al*, 1994; Niemeyer *et al*, 1997; Isomura *et al*, 2003; Tartaglia *et al*, 2003; Loh *et al*, 2004). We investigated the prevalence of mutations in the *PTPN11* gene in children with JMML ($n = 15$) and MDS ($n = 8$). We detected *PTPN11* mutations in 47% of the cases with JMML and 0% of those with MDS. One patient with *p15* hypermethylation also showed *PTPN11* mutation (case J10). It is possible that the hypermethylation of *p15* is coincidental with mutation of *PTPN11* and may not be a critical event in JMML, although further investigation is still needed to clarify whether they cooperate in pathogenesis.

It is known that in a subset of patients with JMML, the disease progresses with an increase in the number of blasts, evolving into AML, a condition referred to as blastic crisis and seen in patients with chronic myeloid leukaemia. We analysed two children with AML who had initially been diagnosed with JMML, and found that *p15* and *p16* were unmethylated in both cases. Although the number of patients was limited, our hypothesis that the aberrant methylation of cell cycle regulatory genes might contribute to the progression from JMML to AML was not verified in this study.

Wong *et al* (2000) reported that paediatric patients with acute leukaemia carrying *p15* hypermethylation had a chromosomal aberration more frequently than children without *p15* hypermethylation. In contrast, the association between *p15* methylation and abnormal cytogenetics was not observed in paediatric patients with ALL by Garcia-Manero *et al* (2003). In therapy-related MDS and AML, hypermethylation of *p15* was strongly related to deletion or loss of chromosome arm 7q (Au *et al*, 2003; Christiansen *et al*, 2003). In this study, three of 10 patients (30%) with hypermethylated *p15* and three of 17 (18%) patients with unmethylated *p15* had a chromosomal aberration, respectively, but the difference was not statistically significant ($P = 0{\cdot}387$, Fisher's exact test).

Aberrant promoter CpG island methylation leads to transcriptional silencing, but some investigators reported that aberrant methylation of *p15* in leukaemic cells is not always associated with transcriptional loss (Preisler *et al*, 2001; Teofili *et al*, 2003). We did not find the silencing of *p15* by aberrant methylation in children with MDS and JMML. It might be attributable to heterogeneous patterns and varying density of methylation in leukaemic cells (Cameron *et al*, 1999), or an unknown mechanism other than methylation regulating *p15* expression (Preisler *et al*, 2001).

Stem cell transplantation (SCT) is recognized as the only curative treatment for advanced MDS both in adults and in children, and especially for JMML (Locatelli *et al*, 1997; Manabe *et al*, 2002). Relapse after SCT is a major cause of treatment failure. Demethylating agents, such as 5-Azacytidine and 5-Aza-2′-deoxycytidine (decitabine), are known to reverse aberrant methylation both *in vitro* and *in vivo*. Indeed, these drugs have been tested in several clinical trials in adult MDS and were shown to induce a haematological response (Daskalakis *et al*, 2002; Silverman *et al*, 2002; Issa *et al*, 2004). Since we showed that *p15* was frequently methylated in children with MDS, it is likely that a subset of children with relapsed or resistant MDS may benefit from demethylating agents, as well as adults. In JMML, *p15* hypermethylation was observed in only a few patients. It might be worth assessing the effects of demethylating agents *in vitro*, taking advantage of the availability of a colony assay for JMML to test new drugs (Emanuel *et al*, 2000). We performed a preliminary experiment using decitabine at a concentration of 10^{-5} mol/l. Decitabine demonstrated an inhibitory effect on spontaneous colony growth in a sample from a patient with JMML who had hypermethylated *p15*, whereas the colony growth in a sample from a normal volunteer co-cultured with haematopoietic factors was not inhibited (data not shown).

In conclusion, this is the first study to examine the methylation status of cell cycle regulatory genes in paediatric MDS and JMML. The incidence of aberrant methylation in paediatric MDS was comparable with that in adult MDS. Although hypermethylation in JMML is a rare event, an examination of methylation status and the *in vitro* testing of demethylating agents could identify patients who might benefit from such drugs.